RSC Advances

REVIEW

View Article Online
View Journal | View Issue

Cite this: *RSC Adv.*, 2026, **16**, 16718

Toxic effects of microplastics in aquatic environments and the pathways to sustainable management

Shivani Kumar S. and Dhanaraj Sangeetha *

Environmental hazards caused by untreated synthetic polymer wastes, which are harmful to the environment after being gradually broken down into microsized particles through a number of processes. Many studies focusing on microplastics (particle sizes ranging from 1 to 5 mm) have been published. Recent discoveries of microplastics in the atmosphere of cities, suburbs, and even remote areas raise the possibility that the atmosphere might carry microplastics over long distances. The tiny size of microplastics, compared with that of macroplastics, makes their detection in environmental samples more difficult and necessitates the requirement of more advanced analytical methods. Microplastics have been detected using a wide range of technologies. This extensive review focuses on the Indian Governmental policies regarding plastic pollution and the origin, classification, detection, marine environmental effects and effective treatment strategies of microplastics. In this study, we also discuss the current approaches, research gaps of previous studies and future challenges. This review suggests that the employment of biological methods of deterioration should be prioritised in order to ensure the continued viability of the ecosystem.

Received 19th July 2025
Accepted 10th March 2026

DOI: 10.1039/d5ra05202e

rsc.li/rsc-advances

Department of Chemistry, School of Advanced Sciences, Vellore Institute of Technology, Vellore-632014, Tamil Nadu, India. E-mail: shivanikumar.s2021@vitstudent.ac.in; dsangeetha@vit.ac.in

Shivani Kumar S.

Shivani Kumar S. completed her Master of Science in chemistry at the PSGR Krishnammal College for Women, Coimbatore, Tamil Nadu, in 2021. She is currently a doctoral researcher under the supervision of Professor Dhanaraj Sangeetha at the Vellore Institute of Technology, Vellore. Her PhD research is dedicated to the investigation of marine-derived biocatalysts, focusing on cellulase enzymes as potential agents for the biodegradation of microplastic pollutants. Her work integrates enzymology, polymer science, and environmental chemistry to elucidate the catalytic pathways facilitating polymer depolymerization in marine systems. The overarching objective of her research is to advance enzyme-mediated degradation technologies as sustainable alternatives for mitigating plastic contamination in aquatic ecosystems.

Dhanaraj Sangeetha

Professor Dhanaraj Sangeetha obtained her PhD degree in environmental chemistry from Bharathiar University, Tamil Nadu. She is an endowed CSIR and Marie Curie Research Fellow at the Council of Scientific and Industrial Research, New Delhi and the European Commission, respectively. She has been a faculty member of the postgraduate program in chemistry at VIT University, Vellore, since 2008. She has published patents and Scopus-indexed book chapters in her research field. Her research articles number more than 70 and have been cited more than 1000 times. Dr Sangeetha has research experience in analytical chemistry encompassing environmental, pharmaceutical and phytochemical analysis. She has also extended her research to the field of formulation and evaluation of nanomaterials for environmental and biomedical applications. She is a member of the American Chemical Society and an associate member of the Royal Society of Chemistry.

1. Introduction

The subsurface environment of the ocean is now believed to harbor vast quantities of microplastics, with complex distribution patterns shaped by their sizes, the physical oceanography, and biological interactions. While significant progress has been made in profiling these distributions up to thousands of meters in depth, methodological standardization and sampling campaigns are required to fully understand the dynamics and ecological implications of subsurface microplastics. Microplastics are plastic fragments (1 μm to 5 mm in size), originating from the breakdown of larger debris or released directly (*e.g.*, microbeads and fibers). Although surface ocean microplastics are extensively recorded, subsurface microplastics (below ~50 cm depth) are widely acknowledged as a significant element of marine plastic pollution across the water column, from coastal regions to the abyssal zone. Plastic pollution, particularly caused by micro- and nano-plastics, remains a persistent and escalating environmental challenge despite increased global awareness. Addressing this issue requires coordinated action among governments, industries, scientists, non-governmental organizations, and communities. Integrated approaches that combine policy reform, public education, corporate responsibility, and grassroots initiatives are essential to effectively reduce plastic inputs into marine environments. The ocean plays a critical role in supporting biodiversity, regulating the climate, and ensuring global food security, yet plastic pollution is increasingly compromising these functions. Keystone species, such as oysters and mussels, are especially vulnerable due to their filter-feeding behavior, which exposes them to widespread micro- and nano-plastics. The ingestion of these particles causes physiological stress, oxidative damage, reduced reproductive success, and increased mortality, threatening both the ecosystem stability and seafood safety. The contamination of marine organisms highlights a direct connection between ocean health and human health through food-web transfer. Therefore, protecting marine ecosystems requires a global shift toward long-term environmental sustainability over short-term economic gain. The actions taken to mitigate plastic pollution today will be instrumental in safeguarding marine biodiversity, ecosystem resilience, and human well-being for future generations.

Microplastics have become a pervasive form of marine pollution, linking ocean health directly to human exposure. These particles originate from the fragmentation of larger plastic debris and from primary sources, such as synthetic fibres and microbeads. Once released into the marine environment, microplastics are transported across surface waters, the water column, and sediments, making them widely available to marine organisms.

Marine species ingest microplastics either directly from seawater or indirectly through contaminated prey. Filter-feeding organisms, including oysters and mussels, are particularly vulnerable because they process large volumes of water and accumulate suspended particles. Microplastic ingestion has been associated with physiological stress, oxidative damage, impaired reproduction, and increased mortality in marine organisms, threatening ecosystem stability and seafood safety.

Microplastics can move through marine food webs *via* trophic transfer, ultimately reaching humans through seafood consumption. Bivalves are of special concern because they are often consumed whole, increasing the likelihood of direct microplastic ingestion. In addition to dietary exposure, humans encounter microplastics through drinking water, air, and food packaging. Recent studies have detected microplastics in human blood, lungs, and placental tissues, indicating systemic exposure.

While definitive human health outcomes remain uncertain, emerging evidence suggests that microplastics and their associated chemicals may induce inflammation, oxidative stress, and endocrine disruption. The pathway from the sea to the human body highlights the interconnectedness of environmental and human health. Reducing microplastic exposure requires upstream interventions, including improved waste management, plastic reduction strategies, and coordinated policy action. Addressing marine plastic pollution is therefore essential not only for protecting ocean ecosystems but also for safeguarding long-term human well-being.

Plastic is an umbrella term that refers to a variety of synthetic polymers. These polymers are typically manufactured through the polymerization of monomers derived from fossil fuels like oil or gas.[1] The polymer may be obtained from coal, natural gases, cellulose, or tree latex if it is not derived from oil or gas. Plastics are synthetic organic polymers with a unique set of qualities (versatility, durability, strength, lightness, and transparency) that make them a "unique substance" with numerous applications in industry, building, medicine, and food safety.[2] At the same time, they decay slowly and may remain in the environment for an extended period. Accidental releases and careless disposal cause an unchecked accumulation of plastic debris in the environment, where it may be broken down by airborne agents and carried downstream by rivers before arriving on beaches.[3,4] Different sizes of plastic trash that each have a different density, chemical makeup, colour, and shape reach the ocean.[5] The majority of publications use the term "microplastics" to refer to plastic particles with a longest diameter of 5 mm. There have been suggestions that the phrase "microplastics" be reanalyzed to include only particles smaller than 1 mm and that the word "mesoplastic" be created to encompass objects with a diameter of 1 to 25 mm. Macroplastics are defined by Lambert *et al.* as being >5 mm, mesoplastics as being >5 to >1 mm, microplastics as being >1 mm to >0.1 m, and nanoplastics as being >0.1 m. However, the highest limit of 5 mm is widely recognized since it allows for the inclusion of a wide spectrum of microscopic particles that can be easily eaten by organisms.[6,7] As a result of the tiny size of microplastics, protozoans, marine creatures, and countless filter feeders eat them.

2. Microplastics in the aquatic environment

Microplastics are consumed by amphipods, polychaete worms, barnacles, and sea cucumbers, thereby accumulating in the

food chain.[8,9] The biogenic domain of plants and animals is in danger due to the ubiquitous presence of microplastics in nature and their potent ability to interact with the environment (both biotic and abiotic), according to Green *et al.* and Setälä *et al.*[10,11] The water column, sediments, surface waters, and aquatic ecosystems all have high levels of microplastics.[12] Because of their known prevalence in marine ecosystems, extended residence time, and tendency to be consumed by biota, microplastics might pose a threat to aquatic habitats. Ultimately, microplastics from many sources make their way into aquatic bodies, where they disperse throughout benthic sediment, subsurface water, and surface water, among other locations, decreasing their bioavailability.[13] Microplastics are particles or pieces of plastic that are smaller than 5 mm in diameter and are created when larger plastics break apart.[14,15] Plastics in the marine environment can fracture into smaller particles.[16,17] Microplastics can take the form of foams, foils, pellets, fibers, pieces, and microbeads.[18] Chemically, plastics vary widely. Polyamide (PA), polyethylene terephthalate (PET) and polyvinylchloride (PVC) have higher densities than seawater, which increases sediment settlement rates, whereas low-density polyethylene (LDPE), polystyrene (PS), high-density polyethylene (HDPE), polyurethane (PUR) and polypropylene (PP) have lower densities and may float primarily on seawater.[19,20] According to a recent study, the presence of microplastics in frogs poses potential risks to the health of wetland ecosystems, and the problem was shown to be particularly severe in Bangladesh.[21] The introduction of microplastics into living systems does not stop with animals; it also occurs in human blood and placenta.[22,23] The current environmental issue is entirely due to plastics and their consequences.

2.1. Land-based pathways of microplastic pollution in aquatic ecosystems

The types of plastics or microplastics that are present in aquatic ecosystems originate from land-based sources, not water-based sources. The primary cause of microplastic contamination is human activity, which is heavily reliant on the regular use of plastic items. According to reports, just 2% of primary MPs come from ocean-based activities, whereas 98% come from land-based activities. MPs typically infiltrate aquatic habitats through inadequate waste management, unlawful dumping, and unintentional and unavoidable discharges, including those that occur during construction, industrial activity, farming, home use, and leisure.[3] Microplastics (MPs) in aquatic environments predominantly originate from terrestrial sources, accounting for approximately 98% of primary MPs, compared with just 2% from marine activities. Daily human reliance on plastic items, including packaging, textiles, and consumer goods, fuels this pollution through poor waste handling practices. Ineffective waste management, illicit disposal, and unintended releases during construction, manufacturing, agriculture, household use, and leisure activities introduce MPs into rivers, lakes, and oceans *via* runoff and wastewater. Agricultural practices amplify this influx, as plastic mulching films deployed globally to boost yields by conserving moisture and suppressing weeds fragment into MPs that infiltrate soils and nearby water bodies. Organic fertilizers contaminated with plastic residues further disseminate these particles across terrestrial and aquatic realms.[24–26]

Tourism exacerbates MP accumulation, particularly on beaches, where visitors discard single-use items like bottles, food wrappers, cups, and straws that degrade or wash directly into coastal waters. High-traffic tourist sites show elevated litter levels, such as 205.75 g m^{-2}, in the beaches of Goa *versus* lower amounts in less-visited areas. These pathways heighten human exposure risks, as beachgoers contact MPs during recreation, potentially ingesting them *via* sand or seafood. Overall, land-based dominance underscores the need for enhanced waste infrastructure, biodegradable alternatives, and tourism regulations to curb aquatic MP influx.[27–30]

2.2. Proliferation of plastics and pathways to aquatic pollution

The durability, versatility, and low cost of plastics have driven exponential global production, reaching over 400 million metric tons of waste annually as of 2022, with projections nearing 460 million tons in 2025. Single-use items dominate this surge: approximately one million plastic bottles are sold every minute worldwide, alongside 500 billion bags yearly and vast quantities of straws, fuelling environmental overload, with recycling rates averaging just 9–14% globally. Polyethylene powers food packaging and bags, while polyamides and polyesters underpin synthetic textiles, shedding microfibers during manufacturing, wear, and laundering.[31–33]

Marine debris encompasses any persistent man-made solid waste, such as plastics, metals, glass, paper, or fabric abandoned on coasts, lost at sea, or transported *via* rivers, sewage, wind, or runoff from land (Fig. 1). Plastics comprise the bulk due to their longevity, fragmenting into macro- and microplastics (MPs < 5 mm) that enter waters indirectly through wastewater, industrial effluents, textiles, and daily activities. Primary MPs arise from cosmetics or abrasives, while secondary MPs originate from larger debris breakdown.[34,35]

Wastewater treatment plants (WWTPs) capture MPs variably: preliminary sieves and screens remove 35–59% of coarse particles (>20 μm), grease traps skim floats, and sand traps settle heavies during primary stages, achieving 50–98% efficiency for larger fragments. Nevertheless, finer MPs (0.2–5 mm) evade capture, with diverse shapes (fibers and fragments), sizes, polymers (PE, PP, and PS), and densities persisting in effluents at 0.2–14 MPs per L post-secondary treatment. This underscores the limitations of WWTPs, releasing MPs and thereby augmenting aquatic pollution.[35–37]

2.3. Marine litter and microplastics in coastal and aquatic environments

Marine litter consists of durable, man-made solid materials that enter oceans and coastlines through direct disposal, accidental loss, or indirect pathways like rivers, storm water, and winds. These materials, including plastics, metals, glass, rubber, and textiles, originate from land-based activities, such as poor waste management and tourism, and sea-based sources like fishing

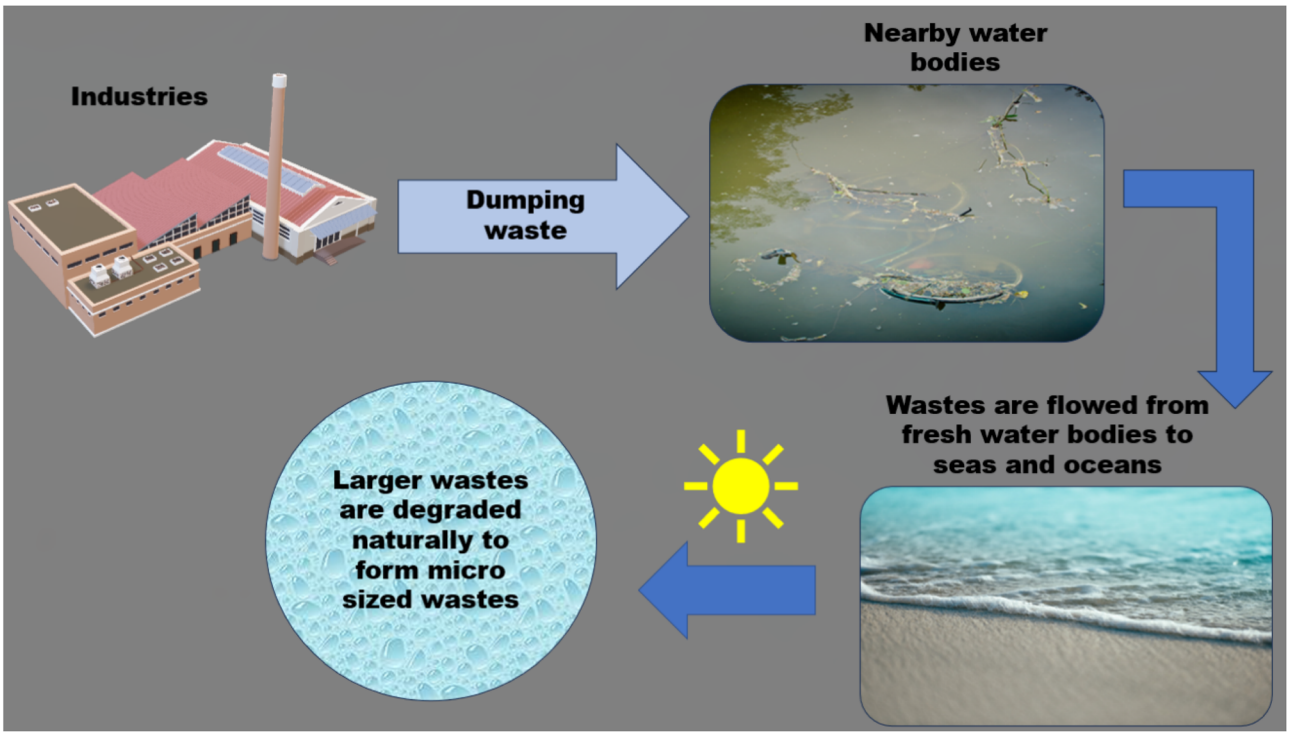

Fig. 1 Transport and distribution pathways of microplastics within and between terrestrial, freshwater, and marine ecosystems.

gear abandonment. Plastics dominate marine debris due to their persistence, comprising up to 86% of beach litter in some regions and posing widespread ecological risks.[38–40]

Microplastics, defined as plastic particles smaller than 5 mm, enter environments primarily *via* wastewater effluents from textile laundering, industrial processes, and urban runoff rather than direct releases. Primary microplastics, such as microbeads from cosmetics or nurdles from manufacturing, are released directly in small sizes, while secondary microplastics are formed from macroplastic fragmentation through weathering and mechanical action. Both types, alongside larger macroplastics, exhibit diverse morphologies including fibres, fragments, films, pellets, and foams.[41,42] Environmental microplastics display high variability in size (from sub-micrometer to 5 mm), polymer type (such as polyethylene and polypropylene), density (0.85–1.4 g cm^{-3}), and shape, influencing their transport, sinking, and bioavailability.[43]

3. Classification and complexity of microplastics

Microplastics are divided into primary and secondary categories based on origin and formation processes. Primary microplastics are generated directly in small sizes from substances like microbeads in cosmetics and toothpastes, plastic pellets or nurdles in industry, and abrasives in blasting or cleaning products. Secondary microplastics arise from the breakdown of larger macroplastics through physical abrasion, UV exposure, and biological degradation in marine and terrestrial settings.[41]

Reports of plastic particles in oceans date back to the 1970s, yet comprehensive studies lagged until the 2000s, with freshwater systems receiving less attention initially. Research surged post-2015, shifting from distribution to toxicity and ecological risks, recognizing microplastics as emerging contaminants due to their ubiquity and persistence.[44] Microplastics exhibit multifaceted characteristics demanding analysis across five key dimensions.[41,43,45–47]

- Size variability from 1 μm to 5 mm, encompassing fragments up to macro scales in some definitions.
- Diverse polymers like polyethylene, polypropylene, and polystyrene, differing in structure, density (0.85–1.4 g cm^{-3}), and degradability.
- Shapes including spheres, fibres, films, foams, and irregular fragments, affecting transport and ingestion.
- Additives, such as plasticizers, flame retardants, UV stabilizers, and pigments, plus sorbed pollutants from weathering.
- Surface properties like charge, hydrophobicity, biofouling, and aging status, altering toxicity between primary and secondary forms.

3.1. Anthropogenic pathways and generation mechanisms of primary and secondary microplastics

Primary microplastics enter environments in small sizes (<5 mm) from direct manufacturing, including nurdles or pellets used in thermoplastic production, microbeads in cosmetics and exfoliants, and microfibers shed during synthetic textile laundering. Tire wear particles from vehicle abrasion represent

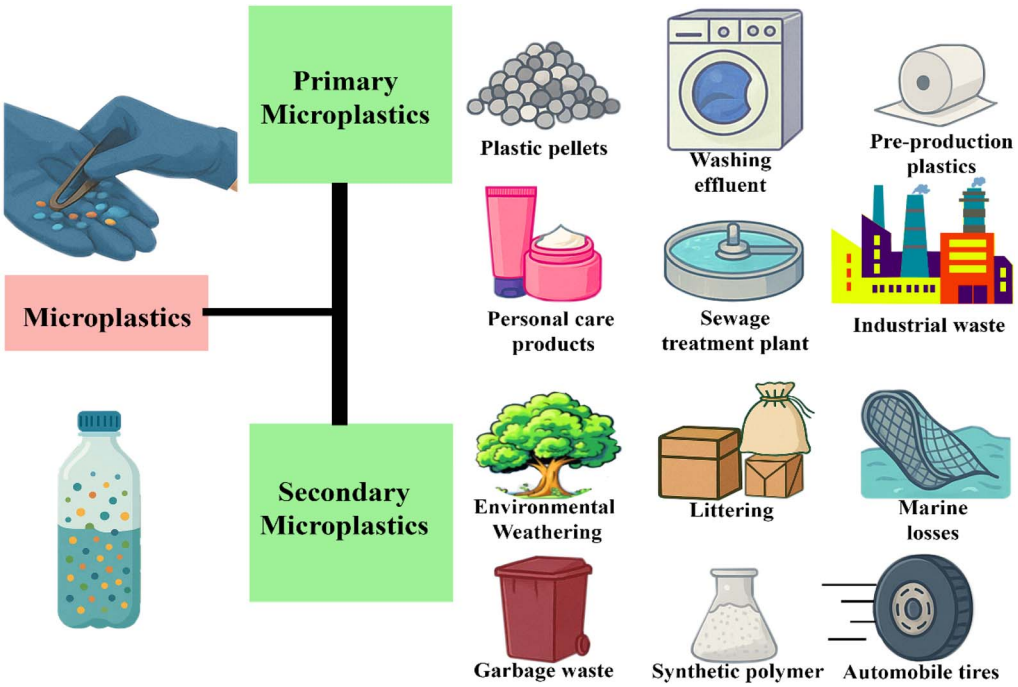

Fig. 2 Schematic of the origin and formation pathways of primary and secondary microplastics from various environmental and anthropogenic sources.

a dominant source, contributing substantially to road dust and urban runoff, while plastic running tracks release fragments *via* wind and precipitation, although emission quantification remains limited. Laundry, detergents, personal care products, and industrial effluents deliver diverse microplastics to wastewater treatment plants (WWTPs), where primary and secondary processes remove 60–96% but discharge residuals directly into surface waters (Fig. 2).[48–52]

Secondary microplastics are formed through the degradation of macroplastics *via* UV photodegradation, mechanical abrasion, wave action, and biofouling, fragmenting items like plastic bags, packaging (39% of global plastic production), and abandoned fishing gear. Despite bans, legacy plastic bags persist as fragmentation sources in urban and riverine areas. Fishing activities contribute significantly, with lost nets, ropes (primarily polyethylene, polypropylene, and nylon), buoys, and polystyrene foams comprising up to 85% of seafloor debris in some regions; such items release fibres through weathering. Maritime accidents further amplify inputs, underscoring fishing gear as a key microplastic originator in oceans. These pathways highlight the ubiquity of microplastics in freshwaters, drinking water, and marine systems, necessitating targeted source controls.[48,53–55]

4. Analytical challenges in microplastic detection

Microplastics, defined as synthetic polymer particles smaller than 5 mm, enter aquatic environments either directly (such as microbeads from cosmetics) or through the breakdown of larger macroplastics exceeding 5 mm in size. Their tiny scale creates formidable barriers to detection and analysis, especially within intricate matrices like sediments, water columns, and biological tissues, where they coexist with vast quantities of natural particulates. Effective sample processing is essential to counter interference from organic matter and minerals, with techniques such as density-based separation, chemical or enzymatic digestion, and precise filtration yielding recovery efficiencies between 70% and 99%, effectively curbing matrix interferences. For polymer verification, particularly at sizes of 1–20 μm, micro-Fourier transform infrared (μ-FTIR) and Raman spectroscopies stand out as premier techniques, despite their labour-intensive nature for high-volume samples; integrating machine learning algorithms now boosts throughput and accuracy in spectral matching. Rigorous protocol standardization, encompassing recovery validations and blank controls, is vital to eliminate quantification biases, thereby enabling credible evaluations of these widespread pollutants. Such comprehensive strategies overcome detection constraints, laying the groundwork for thorough environmental impact studies.[56–59]

4.1. Sampling strategies in marine and sediment environments

Reliable microplastic assessment hinges on disciplined field collection methods targeting particles with sizes below 5 mm, utilizing tools like plankton nets, sieves, and sediment grabs suited to diverse aquatic settings. Sediment protocols lack full harmonization, requiring a clear delineation of benthic (such as riverbeds and lake bottoms) *versus* coastal regimes; the Van Veen grab sampler excels here for its uniform penetration (up to 20 cm) and reproducible yields from consolidated silt or sand layers, although it disturbs softer substrates more than corers.

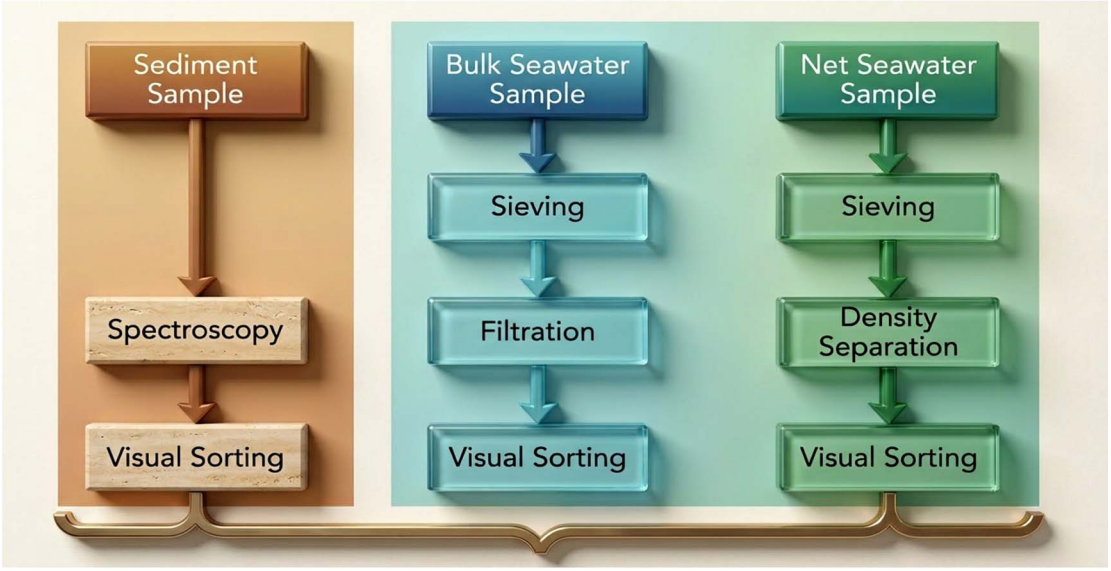

Fig. 3 Different methods used for the preparation, treatment, and analysis of microplastics in sediment, bulk seawater, and net seawater samples.

Preventing contamination demands non-plastic gear (such as stainless steel and glass), limited air exposure, and blank samples to track procedural impurities, even if plastic storage is occasionally necessary.[60]

Water and sediment sampling is divided into three core approaches, *viz.*, selective, bulk, and volume-reduced sampling, each optimized for particle abundance and matrix density.[61]

- Selective sampling focuses on observable macro- and micro-plastics using on-site tools like tweezers or spoons from beaches or sediments, proving efficient for prominent forms, such as pellets or fragments.[61]
- Bulk sampling gathers entire volumes *via* corers or grabs to access hidden or sub-millimetre particles embedded in mud or water, with full laboratory follow-up essential.[61]
- Volume-reduced sampling streamlines capture: beach sieves (500 μm to 5 mm) for surface layers, neuston or Manta nets (200–500 μm mesh) for surface seawater trawls, or finer bongo nets (100–300 μm) for vertical profiles, although smaller meshes risk clogging with fibers.[61]

Nets prevail for aqueous volumes of 1–100 m^3, prioritizing finer meshes (50–200 μm) for microfibers while incorporating replicates and blanks to cap contamination below 5%. These field tactics, paired with lab procedures like digestion, deliver representative data, combining operational speed with analytical fidelity (Fig. 3).[58]

4.2. Laboratory extraction from environmental matrices

Density separation capitalizes on polymer densities, such as polypropylene (0.85–0.94 g cm^{-3}), polyethylene (0.92–0.97 g cm^{-3}), and polystyrene (1.05 g cm^{-3}), to float lighter plastics from heavier sediments using NaCl (1.2 g cm^{-3}), $ZnCl_2$, or K_2CO_3 solutions (1.4–1.8 g cm^{-3}), with agitation or centrifugation over 5–30 minutes and 2–3 cycles securing 85–99% recoveries. Filtered supernatants pass through a 0.7–2.0 μm glass fiber or cellulose membranes under vacuum, capturing over 95% of particles with sizes above 10 μm, often preceded by size-fractionating sieves (500 μm to 5 mm) to segregate macroplastics (>1 mm) and expedite handling.[56–58]

Stereomicroscopy at 10–40× magnification aids initial sorting using traits like colour, transparency, and pliability, yet incurs up to 30% misclassification for particles with sizes under 500 μm, necessitating confirmatory Raman or FTIR scans. Organic removal precedes this step *via* H_2O_2 (10–30%, 24–72 hours), proteinase-K, or alkaline treatments to unmask synthetics. Automated focal plane array systems in μ-FTIR or Raman analyses now scan full filters at 5–50 μm resolution, bypassing manual bias. Tailored protocols for coarse (>500 μm) *versus* fine fractions (<500 μm) enhance efficiency, with verified recoveries surpassing 90% across sediments, water, and biota.[57,62]

4.3. Spectroscopic techniques for microplastic identification

The identification of microplastics demands stringent purification, followed by high-resolution spectroscopy, as weathered, bio-filmed, or dyed polymers mimic organics or minerals in varied matrices, compounded by inconsistent validations lacking blanks or spikes. Pre-analysis removes organics and inorganics *via* density methods, oxidation/enzymatic digestion, and filtration. Microscopy pre-sorting by morphology is now deemed inadequate alone, owing to 20–30% error rates below 300–500 μm, thereby mandating chemical verification.[57,58,62]

μ-FTIR and Raman spectroscopies form the backbone for non-destructive polymer typing, with ATR-FTIR suiting larger (>500 μm) particles *via* direct contact for polyethylene or polyester peaks. Filter-based μ-FTIR analysis (transmission/reflectance, focal plane arrays) automates mapping at 5–20 μm for polypropylene or polystyrene, linking low-density polyolefins to rapid library matches but struggling with pigments. Raman analysis excels for polar polymers like PVC or polyesters (1–5 μm resolution *via* confocal setups), capturing crystallinity and additives effectively despite fluorescence drawbacks in

biofouled samples; hybrid μ-FTIR/Raman sequences broaden coverage for mixed, aged polyethylene fragments.[56,62]

Thermo-methods like pyrolysis-GC/MS break down polystyrene or polypropylene into diagnostic mass fragments for additive quantification in bulk matrices, strong for mass balances but blind to size distributions. SEM-EDS reveals polyethylene weathering cracks or chlorine in PVC *via* C-dominated spectra *versus* silicates, ideal for ambiguous cases. Machine learning on FPA-μ-FTIR/Raman hyperspectral data, plus standardized blanks, spikes, and libraries, now automates filters, curbing bias and enabling cross-study comparisons for polyethylene-heavy pollution tracking. These methods tie polymer identity, such as buoyant polyethylene, to technique strengths (μ-FTIR speed) and limits (Raman fluorescence), powering source-to-risk linkages.[56,58,62]

4.4. Nanoplastic detection thresholds

Detecting nanoplastics smaller than 1 μm remains challenging due to their size approaching the diffraction limit of optical systems, thereby requiring advanced spectroscopic or mass-based methods. Key issues include high matrix interferences from organic matter, salts, and colloids that cause signal quenching or nonspecific adsorption, and spectral overlaps in weathered plastics where oxidation alters polymer signatures, reducing library matching accuracy.[63–66] Standard FTIR and Raman microscopies struggle below 10–20 μm because of diffraction, with practical limits around 500 nm for optimized nano-FTIR or enhanced Raman setups. Specialized systems like hyperspectral Raman systems achieve ~200 nm resolution, but sensitivity drops in complex matrices, necessitating pre-treatments like digestion.[63,67,68]

4.5. Matrix interference challenges

Environmental samples introduce dissolved organics, proteins, and minerals that adsorb onto nanoplastics, attenuating signals or causing aggregation in techniques like Raman spectroscopy. Filtration, magnetic separation, or oxidative digestion mitigates this, although recovery varies (such as 91% for FTIR spectroscopy in some matrices). Biological matrices exacerbate issues for Py-GC-MS, with interferences limiting detection for polyethylene (PE) and PVC.[64,69,70]

4.6. Spectral overlap in weathered plastics

Weathering *via* oxidation or abrasion modifies FTIR/Raman spectra, decreasing identification accuracy from ~80% to below the 70% threshold without updated libraries. Thermal oxidation shifts peaks, causing mismatches; combined FTIR-Raman approaches improve discrimination of degraded polymers.[65,71,72]

5. Global distribution patterns and ecotoxicological impacts of microplastics in aquatic ecosystems

Microplastics pervade aquatic environments worldwide, from subtropical gyres to polar seas, driven by rising plastic production and transport *via* rivers, winds, and currents, with concentrations varying by human population density and proximity to urban/industrial sources. Abundances span 10^{-4} to 10^{4} particles per m^3, peaking in mid-gyre subsurface layers (top 100 m) and high-latitude zones (>55°N/S), where buoyant fragments accumulate in convergence zones while denser particles sink to depths exceeding 2000 m. Coastal estuaries and circulation hotspots exhibit elevated levels (up to 1–3 items per m^3), acting as sinks for riverine inputs and retaining 94% of buoyant microplastics in systems like Chesapeake Bay, while fibres and fragments dominate (50–80%) in sediments and water columns. Arctic sea ice traps concentrations orders higher than surrounding waters (up to 12 000 particles per L), potentially altering melt dynamics and releasing embedded pollutants.[27,73–77]

Ecological distribution reflects the interplay of physical (waves, friction) and biological (biofouling) processes, fragmenting macroplastics into microfibers (most prevalent in seawater) and pellets, with hotspots in densely populated coasts *versus* remote deep-sea trenches. All freshwater eventually channels to oceans, amplifying marine deposition, where oxidative, photolytic, and microbial degradation further reduce particle sizes, enhancing bioavailability.[78–81]

5.1. Toxicological effects on marine biota

Microplastics inflict multifaceted harm on aquatic organisms through ingestion, entanglement, and chemical transfer, affecting >800 species across trophic levels from phytoplankton to cetaceans. Invertebrates (copepods, mussels), fish, seabirds, turtles, and marine mammals routinely ingest particles mistaken for prey, leading to gut blockages, reduced feeding efficiency (up to 40% biomass loss), starvation, and impaired reproduction evident in smaller clutches and 20–50% hatching failure in exposed zooplankton.[78,82–84]

Entanglement in fibres, nets, or rings causes constriction, drowning, and mobility loss, particularly in seals, turtles, and fish, with mortality rates elevated in nursery habitats (Fig. 4). Ingestion predominates as the primary exposure route, bioaccumulating *via* trophic transfer: phytoplankton adsorb particles, passing to zooplankton, fish, and predators, magnifying concentrations 10–100-fold.[79,84,85]

5.2. Chemical and pathogen vectorization

Microplastics sorb persistent organic pollutants (POPs like PCBs and DDT), heavy metals (Pb and Cd), and plasticizers at levels 10^{6} times seawater concentrations, desorbing in the guts to induce oxidative stress, inflammation, genotoxicity, and endocrine disruption. The "plastisphere" biofilms on particle surfaces harbour pathogens (*Vibrio* spp., *E. coli*), antibiotic-resistant bacteria, and invertebrate larvae, facilitating disease transmission and altering microbial community structures.[84–86] Physiological cascades include energy deficits from lipid depletion, immune suppression, and histopathological damage (such as gill abrasion and hepatic vacuolation), compromising growth, survival, and population dynamics. Long-term exposure disrupts ecosystems: coral abrasion reduces calcification, seagrass smothering alters carbon sequestration, and fish behaviour

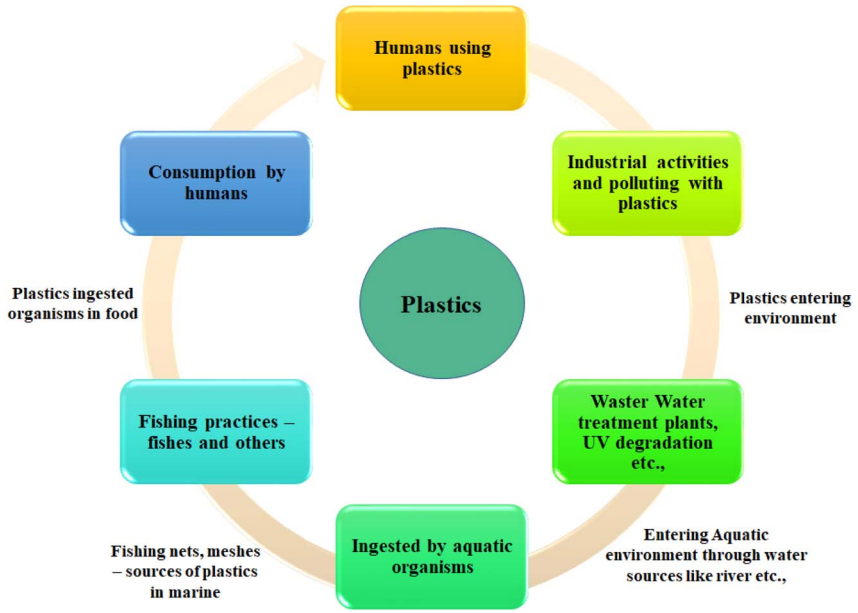

Fig. 4 Cycle of plastic production, usage, and disposal by humans leading to environmental contamination and toxic exposure, ultimately affecting human health.

changes (erratic swimming) heighten predation risk.[76,78,79,83] Despite sentinel studies using marine biota for monitoring, gaps persist in human health linkages *via* seafood and full ecosystem modelling. Urgent needs include standardized risk assessments quantifying bioaccumulation, combined stressor effects (such as with warming), and mitigation *via* source controls to curb proliferation in vulnerable habitats.[27,77,87]

6. Evolving regulatory frameworks for plastic waste management in India

India has implemented a comprehensive regulatory evolution through the Plastic Waste Management (PWM) Rules, initially notified in 2016 and progressively amended in 2018, 2021, and 2022 to address surging plastic pollution, including precursors to microplastics. The 2016 rules mandated waste generators to minimize production, ensure segregated collection, and promote recycling, while assigning responsibilities to urban local bodies (ULBs), retailers, and vendors. Amendments raised minimum carry bag thickness from 40 to 50 microns (2016 baseline), escalating to 75 microns by September 2021 and 120 microns by December 2022, deterring littering by enabling reuse and reducing lightweight discards. The 2018 amendment targeted multi-layered plastics (MLP), phasing out non-recyclable, non-energy-recoverable variants lacking alternative uses, thereby curbing persistent waste streams. By 2022, single-use plastics (SUPs) with low utility and high littering potential, such as plastic sticks for balloons, earbuds, cutlery, plates, cups, straws, and flags, faced outright prohibition effective July 1, 2022, aligning with the vision of Prime Minister Narendra Modi for SUP elimination. These measures encompass ~60% of plastic packaging waste, emphasizing circular economy principles through rigid packaging reuse and mandatory recycling targets under Extended Producer Responsibility (EPR).[88,89]

6.1. Extended producer responsibility and digital compliance infrastructure

EPR, formalized in the 2022 PWM Amendment Rules, shifts end-of-life accountability to producers, importers, brand owners (PIBOs), and processors, requiring registration on the centralized online portal of the Central Pollution Control Board (CPCB), which was launched on March 31, 2022. This platform facilitates EPR certificate issuance, annual return filing, credit trading, environmental compensation levies, and third-party audits, enhancing traceability for flexible/rigid plastic packaging. Recent expansions mandate manufacturers and traders to register, broadening supply chain oversight and enforcing quantified recycling obligations (such as 30–100% by 2025–2030 per polymer category). Non-compliance invites penalties, fostering accountability amid the annual plastic waste generation of 3.5–4 million tonnes in India.

6.2. Complementary national initiatives and awareness campaigns

Beyond statutory rules, India integrates behavioural and infrastructural interventions. The Swachh Bharat Mission (Urban 2.0 and Grameen Phase II) drives plastic segregation, recycling *via* Material Recovery Facilities (MRFs), and reverse vending machines, recycling millions of bottles and creating jobs while cutting CO_2 emissions. Initiatives like India Plastics Pact, Project REPLAN, Un-Plastic Collective, and Go Litter Partnerships promote industry-led reuse, upcycling, and litter prevention, supported by state bans (such as Sikkim, Himachal Pradesh). Urban innovations include the vendor campaigns

against SUPs in Trichy, milk pouch buy-back schemes in Andaman, and MRFs processing 10–65 tonnes daily into chipboards, bolstering circularity. These align with global SDGs, emphasizing community engagement under "Swabhav, Swachhata, Sanskar".

6.3. Microplastic bioaccumulation and ecotoxicological ramifications

PWM regulations indirectly mitigate the accumulation of microplastics by curbing macroplastic inputs, yet bioaccumulation in marine biota underscores urgency. Direct exposure (bathing) and trophic transfer expose crustaceans (*Artemia franciscana*), zooplankton, bivalves, fish, and larvae to particles mimicking prey, impairing adhesion to exoskeletons, ingestion, growth (20–50% reduction), metabolism, reproduction (delayed molting, smaller clutches), and cellular functions (oxidative stress, genotoxicity). Low-nutrient filter-feeders like *Artemia* ingest density-matched microplastics, passing contaminants up food webs to seafood consumed by humans.[83–85,87]

Bioassays reveal dose-dependent effects including polystyrene microbeads alter sea squirt/copepod larvae settlement, mussels exhibit pseudofeces production and energy deficits, while fish display hepatic inflammation and behavioural anomalies. Chronic exposure *via* contaminated sediments or water columns exacerbates risks in the coastal ecosystems of India, where SUP bans aim to stem fragmentation sources. Rigorous monitoring and EPR enforcement remain pivotal to severing these pathways, safeguarding aquatic health and human consumers.[78,82,83,87]

7. Abiotic and biotic degradation pathways of synthetic polymers in aquatic environments

Synthetic polymers exhibit exceptional environmental persistence, resisting rapid breakdown and persisting for centuries in marine systems, where fragmentation into microplastics facilitates ingestion by aquatic biota and trophic transfer into food webs. Degradation proceeds *via* abiotic (physical, photochemical, chemical) or biotic mechanisms, fragmenting polymers into oligomers, monomers, or mineralized by-products while progressively reducing particle size (Fig. 5).[55,67,90]

Physical fragmentation dominates initial breakdown through mechanical abrasion (wave action, sediment scour), thermal cycling, and freeze-thaw stresses, generating secondary microplastics from macro-litter without altering chemical structure. Photodegradation initiated by UV-B/C radiation (290–400 nm) induces chain scission, crosslinking, and carbonyl formation in polyolefins (PE, PP), embrittling surfaces for subsequent mechanical failure; surface layers degrade 10–100× faster than interiors owing to oxygen diffusion limits.[55,75,78]

Chemical hydrolysis targets ester/amide bonds in polyesters (PET) and polyamides (nylon), while thermo-oxidative reactions generate peroxides and hydroperoxides, accelerating fragmentation in oxygenated waters. Biotic degradation involves microbial consortia (bacteria like *Ideonella sakaiensis*, fungi, algae) secreting extracellular enzymes (cutinases and lipases) that hydrolyze surface polymers, although rates remain low (<1% mass loss per year) for recalcitrant polyolefins.[55]

7.1. Advanced remediation technologies for microplastic mineralization

Recent innovations harness photocatalysis, electrocatalysis, and bio-affinity for targeted microplastic degradation. Ariza-Tarazona *et al.* (2019) demonstrated TiO_2-mediated photocatalysis mineralizing 90% of high-density polyethylene (HDPE) microbeads from commercial cleansers under UV-A, producing CO_2 and low-molecular-weight acids.[91] Tofa *et al.* (2019) advanced visible-light ZnO nanorod photocatalysts, achieving 60% weight loss and 80% defluorination of low-density polyethylene (LDPE) fragments *via* –OH and h^+ radicals.[92]

Electrochemical approaches excel for halogenated polymers: Miao *et al.* (2020) combined cathodic de-chlorination with anodic –OH generation, degrading 70% of polyvinyl chloride (PVC) microplastics while recovering Cl^- ions.[93] Magnetic carbon nanotubes functionalized by Tang *et al.* (2021) adsorbed 95% of polystyrene microbeads from dilute suspensions, enabling magnetic recovery and reuse.[94]

Bioengineered anchor peptides selectively bind polyethylene, polypropylene, and polyurethane, facilitating enzymatic degradation or flocculation in low-concentration matrices. Bismuth oxychloride (BiOCl) hydroxyl-enriched nanosheets photocatalytically mineralize polyethylene 24× faster than bulk plastics under simulated sunlight *via* oxygen vacancies that enhance charge separation. These heterogeneous catalysts achieve >80% mineralization efficiency, outperforming biotic rates by orders of magnitude, although scaling remains challenging owing to aggregation and real-matrix interferences. Integration with wastewater treatment holds promise for source control, curbing microplastic proliferation.[95,96]

7.2. Photocatalytic and electrochemical strategies for microplastic mineralization

Microplastic degradation proceeds through coupled photooxidative, catalytic, and enzymatic steps in which surface functionalization, chain scission, and mineralization are tightly linked to polymer structure and reaction conditions. Molecular-scale interactions among microplastics, reactive oxygen species (ROS), and enzymes govern adsorption, bond cleavage, and overall degradation kinetics.[97,98]

Microplastics resist conventional biodegradation due to their high molecular weight and chemical inertness, necessitating advanced oxidation processes (AOPs) for chain scission and mineralization. Photocatalysis employs semiconductor catalysts (TiO_2, ZnO, BiOCl, and g-C_3N_4) activated by photons exceeding their bandgap energies (2.5–3.2 eV), generating electron–hole pairs that produce reactive oxygen species (ROS): hydroxyl radicals (–OH, $E^\circ = 2.8$ V), superoxide (O_2^-), and holes (h^+). These species initiate non-selective oxidation, cleaving C–C/C–H bonds in polyolefins (PE, PP, PS), yielding carbonyls,

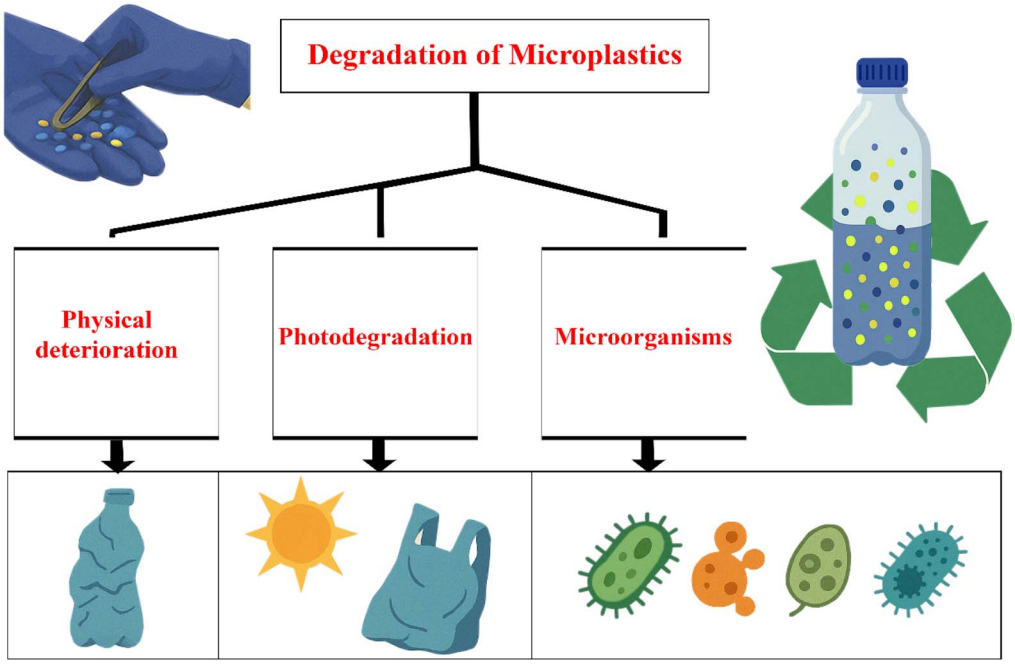

Fig. 5 Schematic of the sustainable and environmentally friendly methods used for the degradation of microplastics.

carboxylic acids, and ultimately CO_2/H_2O; HDPE achieves 60–90% mass loss after 24–48 h under UV-A/visible light.[67,99]

Efficiency hinges on UV/visible light sources (λ < 400 nm optimal), high-surface-area catalysts (nanorods/sheets >100 m^2 g^{-1}), and polymer properties, where crystalline PP degrades more slowly than amorphous PS owing to its higher packing density. Oxygenated aquatic matrices enhance O_2^- formation, while a pH of 3–7 maximizes –OH stability; visible-light variants (doped ZnO and BiOCl) reduce energy demands.[96,99,100]

Electrochemical degradation applies potentials (2–10 V) across electrodes to oxidize water/anions, generating site-specific ROS at anode surfaces. Boron-doped diamond (BDD) and Ti/Pt anodes produce physisorbed –OH *via* water discharge (equation: $H_2O \rightarrow {}^{\bullet}OH + H^+ + e^-$), achieving 70–95% PVC/PS defluorination/de-chlorination *via* direct electron transfer and indirect radical attack. Chloride media produce hypochlorite/Cl^- for halogenated polymers, whereas bubble-induced micro-jetting mechanically breaks apart particles. Current density (10–100 mA cm^{-2}), electrode durability (BDD > TiO^2), and microplastic dispersion—sub-100 μm particles degrade 3–5× quicker *via* accelerated mass transfer—are important factors.[93,100,101]

Photocatalysis excels in sustainability (solar potential) but faces recombination losses (η < 20%), while electrochemistry offers process control yet incurs 5–20 kWh kg^{-1} costs. Hybrid photo-electro systems merge advantages, achieving >95% PS removal.

7.3. Emerging biotechnological and physicochemical approaches for microplastic remediation

For microplastics, traditional waste management is challenging due to their recalcitrant polymer structures, prompting diverse degradation strategies beyond photocatalysis and electrochemistry. Enzymatic biodegradation leverages microbial hydrolases, including PETase/MHETase from *Ideonella sakaiensis*, cutinases (such as CALB, *Humicola insolens*), lipases, to cleave ester/amide bonds in PET, achieving 90% depolymerization to monomers (TPA, EG) at 30–70 °C; engineered variants boost activity 10–100× *via* directed evolution. Bacterial (*Pseudomonas*, *Bacillus*, *Rhodococcus*) and fungal (*Aspergillus*, *Fusarium*) consortia degrade PE/PP (0.5–8% weight loss/30–90 days), forming biofilms that secrete oxidases, although polyolefins resist owing to their hydrophobicity.[102–104]

Bacillus cereus strains stand out for scale-up due to consistent 20% degradation in 30 days across soil/wastewater sources, robust biofilm formation enhancing adhesion, and ambient conditions (26–37 °C, neutral pH). *Bacillus paramycoides* shows similar efficiency on LDPE from dumpsites, and this is adaptable to soil bioremediation. Deep-sea *Bacillus velezensis* offers potential for polyurethane but requires cold adaptation for terrestrial use. Fungal systems, like *Aspergillus*, lag behind in speed/extent compared with the aforementioned bacteria. Co-cultures could increase rates beyond 25%, as seen in recent LDPE trials.[105–109] Advanced oxidation processes (AOPs) like Fenton (Fe^{2+}/H_2O_2) and ozonation generate –OH for non-selective chain scission; thermal-Fenton variants mineralize 76–96% PE/PS in 12–16 h at 90–120 °C, with pre-treatment *via* chain stretching. Ultrasound cavitation induces acoustic streaming, micro-jetting, and pyrolysis hotspots (5000 °C, 200 MPa), fragmenting PVC/PE (38–90% removal/5–360 min) through density-dependent agglomeration/sedimentation.[102,110–113] Thermal pyrolysis thermally cracks polymers (400–600 °C) into monomers/oils/gases; mixed PP/PET/PVC yields synergistic T_{max} shifts (630–950 K), producing alkenes and carboxylics *via* carbonyl intermediates. These methods complement each other, with bio-enzymes offering

selectivity and AOPs/pyrolysis speed.[114,115] Biotech excels in eco-compatibility but lags behind in kinetics; AOPs/ultrasound suit wastewater, and pyrolysis enables upcycling despite emissions. Hybrids (enzyme-AOP) promise >95% efficiency.

7.4. Molecular interactions and structural relationships

Enzymes such as PETase, cutinases, lipases, and cellulases first adsorb to the hydrophobic microplastic surface *via* hydrophobic patches and complementary charge distributions and then recognize ester or amide bonds within amorphous domains. Photo- and Fenton-type catalysts instead interact by generating ROS (–OH, O_2^-, $^1O_2$) that attack C–C and C–H bonds, introducing carbonyl, hydroxyl, and carboxyl groups that increase surface polarity and enzyme accessibility.[116]

Polymer crystallinity, glass-transition temperature, and aromaticity strongly influence susceptibility: amorphous PET and PS regions degrade faster than highly crystalline PE or PP, and photoaging that increases O-containing groups enhances hydrogen bonding with water and co-contaminants.[117]

7.5. Degradation mechanisms and reaction schemes

Photooxidation typically follows initiation, propagation and termination steps in which chromophore excitation or catalyst-generated –OH abstracts H-atoms, forming macroradicals that react with O_2 to yield peroxyl radicals and hydroperoxides, which decompose into shorter chains and carbonyl-rich fragments. In catalytic Fenton and photocatalytic systems, Fe^{2+}/Fe^{3+} or semiconductor interfaces accelerate ROS formation, driving successive chain scission and partial mineralization to CO_2 and small organics.[98,118]

Enzymatic pathways proceed *via* the nucleophilic attack of an active-site serine or water molecule on ester bonds, passing through tetrahedral intermediates and releasing soluble monomers or oligomers, such as MHET and terephthalic acid for PET, or oligomeric fragments for other polyesters. Recent protein engineering has strengthened substrate-binding clefts and increased hydrophobic contacts, improving PETase catalytic efficiency and enabling activity at environmentally relevant temperatures.[119]

7.6. Kinetic data and mechanistic insights

Photocatalytic microplastic degradation often follows apparent pseudo-first-order kinetics, with rate constants increasing with UV intensity, catalyst loading, and surface area, and decreasing with particle size and crystallinity. Reported systems, such as Ag/TiO_2 or doped TiO_2/ZnO, have achieved near-complete PE microplastic mass loss under optimized UV conditions, highlighting the importance of particle size (125–150 μm) for maximizing radical-polymer contact.[98,120–122]

Enzymatic degradation rates are usually limited by surface erosion; kinetic analyses show Michaelis–Menten behaviour, where k_{cat}/K_m improves with engineered binding interfaces and increased amorphous content of the plastic substrate. Coupled catalytic–biocatalytic schemes demonstrate that prior photooxidation or Fenton treatment accelerates subsequent enzymatic hydrolysis by increasing surface roughness and introducing accessible functional groups, pointing to synergistic hybrid processes for microplastic remediation.[119,123]

8. Factors affecting degradation

8.1. Enhanced degradation rates

Explicit first-order rate constants (k) improve comparability across methods. For biological degradation, mangrove bacteria yield $k = 0.006$–0.010 day^{-1} for polymers like PVC ($k = 0.0074$ day^{-1}, $t_{1/2} = 93$ days) and PHB, with PA being the most recalcitrant. Photocatalytic processes using TiO_2 under UV report pseudo-first-order $k \approx 0.01$–0.05 h^{-1} for PE and PS films, achieving 60–90% mass loss in 24–72 h, although crystalline PP shows lower k owing to light penetration limits (Table 1). Electrochemical oxidation delivers k up to 0.1 h^{-1} for PS at 16.3 A m^{-2}, with 92–97% removal.[124–126]

8.2. Energy comparisons

Normalizing to kWh kg^{-1} microplastic reveals stark trade-offs. Electrocoagulation requires 15–30 kWh m^{-3} (≈5–20 kWh kg^{-1} at typical 1 g L^{-1} loadings), driven by electrode scaling but offset by sludge issues. AOPs like Fenton require 10–50 kWh kg^{-1} for 76–96% mineralization, factoring in reagent costs and 25–120 °C heating. Ultrasound cavitation uses 200–500 W (≈2–10 kWh kg^{-1} for 38–90% removal in hours), while solar photocatalysis approaches near-zero net energy in thin-film setups.[126,130]

8.3. Mineralization *vs.* fragmentation

Distinguishing complete mineralization (to CO_2/CH_4) from fragmentation (to <5 μm particles) is critical, as fragments may persist as nanoplastics. Enzymatic methods achieve partial mineralization (1–90% mass loss over months, PET > PE) *via* hydrolase cleavage to non-toxic monomers, minimizing fragments. AOPs and photocatalysis excel in mineralization (70–96% to CO_2/acids) but risk initial fragmentation if radicals cause uneven chain scission. Cavitation favours fragmentation (shear/micro-jetting), with only 38–90% true mass loss and density-driven trends (PVC > PE). Pyrolysis converts >95% into volatiles but requires emission controls.[126,131,132]

8.4. Scalability analysis

Beyond qualitative notes, scalability hinges on cost ($ per kg), throughput, and integration. Biological methods scale *via* WWTP bio stimulation (enzyme production costs dropping 20–50% yearly), handling 10–100 kg m^{-3} day^{-1} but over months. Electrochemical/electrocoagulation scales linearly with electrode area (to tons/day in flow reactors) at $0.10–0.30 per m^3, although energy (15–30 kWh m^{-3}) limits it to sludge-heavy sites. Photocatalysis requires micromotor or dynamic membrane reactors for light penetration, projecting 1–10 tons per day at <$0.20 per kg with solar input. Pyrolysis is industrial-ready (such as >100 tons per day plants), but emissions demand 30–50% higher capex. Overall, hybrid AOP-bio systems offer the best pilot-to-commercial transition (Table 2).[124,130,132]

Table 1 Technique comparison table

Polymer class	Technique	Detection limit	Quantitative capability	Major limitation
PS and PE	FTIR	~10–20 μm particles	Particle counting; semi-quantitative	Diffraction limit <1 μm; matrix interference spectroscopy[63]
PS and PMMA	Raman	~200–500 nm particles	Particle counting; low mass accuracy	Fluorescence; long acquisition[66,68]
PS, PE, and PVC	Py-GC-MS	0.01–2.6 μg mass	High (mass-based)	Matrix effects in bio/samples; not for PE/PVC[127]
General MPs	SEM-EDS	~5 μm particles	Elemental ID; qualitative	No molecular ID; time-intensive[128,129]

9. Quantitative degradation metrics

The degradation efficiencies of microplastics vary significantly across methods like UV photodegradation, microbial biodegradation, photocatalysis, and advanced oxidation processes (AOPs), with quantitative metrics revealing slower natural processes compared with engineered treatments.

9.1. UV photodegradation rates

UV exposure drives the fragmentation of microplastics into nanoplastics and dissolved organics, with pseudo-first-order rates for polyamide-6 (PA-6) at 2.6×10^{-7} h^{-1} (10–150 nm fragments), 9.4×10^{-8} h^{-1} (40–800 nm), and 2.4×10^{-7} h^{-1} (300–5000 nm), plus 6.3×10^{-6} h^{-1} for dissolved organics. Annual mass loss equivalents reach 23.1 mg g^{-1} $year^{-1}$ for PA-6 dissolved organics and 0.951 mg g^{-1} $year^{-1}$ for 10–5 μm fragments, while thermoplastic polyurethane (TPU_ether_arom) shows 7.8 mg g^{-1} $year^{-1}$ for organics and 0.589 mg g^{-1} $year^{-1}$ for fragments.[98]

9.2. Microbial mass loss

Bacterial strains achieve modest weight reductions over weeks to months: *Rhodococcus* sp. yields 4.0% polyethylene (PE) loss in 40 days, *Bacillus* sp. yields 6.4% PE loss in 40 days, and *Pseudomonas aeruginosa* yields up to 20.0% low-density PE (LDPE) loss in 120 days. Fungal and consortia efforts typically fall within the range of 0–15% overall, limited by slow kinetics and incomplete mineralization.[126]

9.3. Photocatalytic efficiencies

N-doped TiO_2 photocatalysis under visible light induces notable mass loss in polyethylene variants: high-density PE (HDPE) and LDPE show degradation after 50 hours at a pH of 3, with smaller particles exhibiting higher rates owing to the increased surface area. Polystyrene and polymethylmethacrylate nanoparticles reach ~50% carbon loss *via* TiO_2–P25/βSiC composites.[133]

9.4. AOP energy metrics

Thermal Fenton AOPs degrade ultrahigh-molecular-weight PE with 95.9% mass loss in 16 hours and 75.6% mineralization in 12 hours, driven by hydroxyl radical synergy under hydrothermal conditions (energy input not explicitly per gram but implied high *via* rapid processing). Photocatalytic HDPE systems achieve 71.77% mass loss at an acidic pH of 3 and 0 °C (Table 3).[111,134]

10. ROS-mediated mechanisms

ROS-mediated mechanisms in microplastic degradation involve reactive oxygen species (ROS) like hydroxyl radicals (–OH) and superoxides, which drive oxidation *via* chain reactions, but their thermodynamic feasibility varies by polymer type and environmental conditions. Higher crystallinity restricts chain mobility, slowing ROS access and reducing rate constants by up to 20-fold in amorphous *vs.* crystalline polymers. The shift from fragmentation to mineralization depends on a sustained ROS attack, cleaving chains into oligomers small enough for microbial assimilation or complete CO_2 release.[111,119,135–138]

10.1. ROS thermodynamics

ROS such as –OH ($E^\circ = 2.7$ V *vs.* NHE) and SO_4^- ($E^\circ = 3.1$ V *vs.* NHE) initiate hydrogen abstraction and C–C scission, but thermodynamic barriers arise in the basic autoxidation scheme (BAS) owing to endothermic propagation steps. Revised BAS accounts for defects in hydrogen abstraction energetics, with photoaging favouring PE/PS/PET *via* exergonic ring opening or decarboxylation under UV. Hydrothermal Fenton enhances feasibility by protonating chains, forming hydroperoxides that split exothermically into new radicals.[111,137]

10.2. Crystallinity impact

Crystalline regions limit molecular mobility and water/ROS diffusion, yielding rate constants 20 times lower than those of amorphous phases (such as PDLLA *vs.* PLLA hydrolysis). In UHMW-PE, initial oxidation unfolds chains, boosting crystallinity temporarily (74% to 81%) before carbonyl insertion disrupts packing, dropping it to 4% and increasing rates ($k_1 = 0.006$ h^{-1} to $k_2 = 0.30$ h^{-1}). Higher crystallinity correlates inversely with amorphous fraction (I_a/I_b ratio in FTIR), slowing –OH attack.[111,137,138]

Table 2 Comparative overview of microplastic degradation technologies: mechanisms, efficiency, scalability, and environmental implications

Aspects	Photocatalytic degradation	Electrochemical degradation	Enzymatic/biological	AOPs (Fenton/ozone)	Ultrasound cavitation	Thermal pyrolysis
Mechanism	Photon-induced generation of reactive species (–OH, O_2^-, $^1O_2$, h^+) causing chain scission and oxidation	Electron-driven formation of adsorbed oxygen, –OH, O_2^-, and Cl^-; anodic oxidation	Hydrolase-mediated cleavage and oxidative biofilm action	–OH and SO_4^- radicals induce polymer chain fragmentation	Cavitation-induced shear, micro-jetting, and localized pyrolysis	Thermal cracking of polymers into volatiles and condensable fractions
Reactive species	–OH, O_2^-, $^1O_2$, and h^+	–OH, Cl^-, O_2^-, and adsorbed oxygen	ROS from microbial metabolism	–OH and SO_4^-	–OH and localized heat zones	Thermal radicals (C^- and H^-)
Energy source	UV or visible light (solar-compatible)	Electric potential (2–20 V DC)	Ambient – 70 °C and biological energy	Chemical reagents (H_2O_2, Fe^{2+}, and O_3) and 25–120 °C	Mechanical/ultrasound input (200–500 W)	External heat (400–600 °C)
Efficiency	60–90% mass loss (24–72 h; polymer-dependent)	70–95% mineralization (broad-spectrum)	1–90% mass loss (days–months; PET > PE)	76–96% mineralization (hours)	38–90% removal (minutes–hours; density-dependent)	>95% conversion (minutes)
Polymer specificity	Crystalline polymers like PP resist and UV-absorbing polymers degrade faster	Surface-dependent; halides enhance efficiency	PET and PU degrade easily, and PE and PP degrade slower	Broad-spectrum; crystalline polymers more resistant	PVC > ABS > PE (density-driven trends)	PP, PET, and PVC degrade synergistically
Scalability	Limited by light penetration; and requires optimized reactor geometry	Scalable with electrode area; energy-intensive in continuous flow	Dependent on enzyme cost and production; field application feasible	Suited for WWTP integration; requires reagent dosing	Adaptable to flow reactors	Industrially scalable; emission control needed
Environmental fit	Effective in thin-film or coating systems; solar-driven	Integrable with WWTP/sludge treatment	Environmentally benign; biodegradable products	Chemical residues/sludge management required	Fragmentation risk to microplastics	Produces recoverable oils/gases; needs emission treatment
By-products	CO_2 and oxidized fragments	CO_2, acids, and sludge	Monomers and non-toxic compounds	CO_2, acids, and sludge	Fragments (may remain partially degraded)	Oils and gases (recoverable, valuable fraction)

Table 3 Key comparisons[a]

Method	Polymer example	Mass loss (%)	Time	Rate constant or notes [source]
UV photodegradation	PA-6	23.1 mg g^{-1} $year^{-1}$ (organics)	1 year equiv.	6.3×10^{-6} h^{-1} for organics[98]
Microbial	LDPE	20%	120 days	Bacterial (*P. aeruginosa*)[126]
Photocatalytic	HDPE/LDPE	Variable (high for small sizes)	50 h	Visible light, pH = 3 (ref. 133)
Thermal Fenton	UHMW-PE	95.9%	16 h	–OH radicals[111]

[a] These metrics highlight AOPs and photocatalysis as faster for sustainable management, while natural UV/microbial paths contribute modestly to long-term aquatic breakdown.[111]

10.3. Fragmentation–mineralization transition

Fragmentation dominates early *via* surface oxidation and chain scission into oligomers, governed by ROS-induced carbonyl formation and hydrophilicity increase. Mineralization requires an oligomer size below 600 Da for cellular uptake, followed by enzymatic hydrolysis to CO_2/H_2O; incomplete ROS persistence leads to persistent fragments. TiO_2 photocatalysis achieves full PS mineralization (TGA confirmation) *via* e_{CB}^-/h_{VB}^+, generating –OH for exhaustive C–C cleavage (Table 4).[119,126,135]

11. Role of bond energies, backbone structures, crystallinity, and oxidation pathways in microplastic degradation

The long-term persistence of microplastics (MPs) in aquatic environments stems largely from the intrinsic chemical stability of common polymers, such as polyolefins (polyethylene, polypropylene) and polyesters (polyethylene terephthalate, PET). A mechanistic understanding of bond strengths, backbone design, and crystallinity helps explain why some plastics resist degradation while others can be targeted *via* oxidation, hydrolysis, or photocatalysis, which in turn influences both toxicity (*via* leaching and fragmentation) and prospects for sustainable management.[82,139–141]

11.1. Bond energies and backbone structures

Polyolefin backbones consist mainly of strong C–C and C–H bonds whose homolytic bond dissociation energies (BDEs) typically exceed 350–400 kJ mol^{-1}, making them highly resistant to thermomechanical and oxidative attack under ambient conditions. In contrast, PET and other polyesters contain C–O and ester (R–COO–R′) linkages; the ester BDE is lower (~330–360 kJ mol^{-1}) and more polar, rendering them more susceptible to nucleophilic attack by water or enzymes, especially at elevated temperatures.[140–142]

Introducing "weak" or cleavable linkages, such as esters and ketones, or unsaturation into otherwise saturated polyolefin backbones strategically lowers the effective activation barrier for chain scission while preserving mechanical performance. For instance, ester-functionalized polyethylene (HDPE-DM and LLDPE-DM) can be depolymerized at around 120 °C, drastically reducing energy demand *versus* conventional pyrolysis, thereby opening pathways for chemical recycling instead of slow, uncontrolled abiotic oxidation in aquatic systems.[141,143]

In the context of this review, this implies that future sustainable polyolefin design should favour backbone architectures with strategically placed labile bonds that resist wear during service life but become accessible to hydrolysis or catalyzed oxidation when discarded, thereby shortening microplastic lifetimes and mitigating long-term toxicity.[140,141]

11.2. Effects of crystallinity on degradation and toxicity

Crystallinity governs the physical accessibility of oxygen, water, and reactive species to polymer chains, thereby modulating the rate and mechanism of microplastic aging. In polyethylene, higher crystallinity reduces free-volume pathways for O_2 diffusion, slightly slowing initial oxidation but simultaneously favouring cross-linking and carbon-chain growth over chain scission, which can prolong the existence of larger, more persistent fragments. Conversely, lower crystallinity enhances chain mobility and oxygen penetration, promoting more extensive chain breakage and faster formation of smaller, more oxidized fragments that may leach more readily into aquatic media.[139,144,145]

For PET-based microfibers, high crystallinity similarly restricts ester–ester hydrolysis and enzymatic access, explaining why bottles and textiles persist longer than amorphous films. Recent studies on reactive molecular dynamics show that PET hydrolysis begins with backbone ester cleavage, yielding bis-(2-hydroxyethyl) terephthalate (BHET) and mono-(2-hydroxyethyl) terephthalate (MHET), which further hydrolyze to terephthalic acid (TPA) and ethylene glycol (EG); these intermediates can then either repolymerize or diffuse into the environment, contributing to chemical toxicity.[142]

Table 4 Quantitative overview

Aspect	Crystalline	Amorphous	Governing factor [source]
Rate constant ratio	Baseline	Up to 20× faster	Mobility/ROS access[138]
Crystallinity change (PE)	+7% initial, then −70%	N/A	Chain unfolding to carbonyl disruption[111]
Transition threshold	Oligomers >600 Da (fragments)	<600 Da (mineralizable)	Size for bioassimilation[111]

11.3. Ester hydrolysis pathways in PET-based microplastics

PET backbone degradation in aquatic settings proceeds *via* stepwise ester hydrolysis, with both abiotic and biotic routes converging on similar mechanistic schemes. In chemical hydrolysis, water attacks the ester carbonyl, forming a tetrahedral intermediate that collapses to a carboxylic acid (TPA end) and a hydroxyl-terminated oligomer; repeated cleavages yield MHET, BHET, TPA, and EG, with TPA and EG being the dominant low-carbon products.[142]

12. Mechanistic pathways

Enzymatic PET hydrolysis shares this core esterolytic motif but adds substrate selectivity and surface erosion. Recent pathway analyses of PET-hydrolases show that breakdown proceeds first *via* heterogeneous attack on the polymer surface, generating oligomers that then undergo homogeneous solution hydrolysis in the bulk phase. The autohydrolysis of intermediates, such as EG and EG-containing oligomers (such as TPA–EG), further feeds the network, sometimes generating additional reactive species that may catalyze more rapid degradation or contribute to secondary pollution.[142,146]

In the context of toxicity, these hydrolysis pathways release monomers and small oligomers (TPA, EG, MHET) that can disrupt osmoregulation, metabolic pathways, and endocrine functions in aquatic organisms, while remaining solid fragments act as vectors for heavy metals and persistent organic pollutants. Sustainable management can therefore leverage controlled hydrolysis (such as in chemical recycling or engineered bioreactors) to transform PET MPs into closed-loop feedstock rather than allowing uncontrolled, slow hydrolysis in open water.[82,139,141,142]

12.1. Radical propagation in photocatalytic polyolefin oxidation

The photocatalytic degradation of polyolefin microplastics (for example, PE and PP) in aquatic environments follows a radical-chain autoxidation mechanism initiated by photogenerated reactive oxygen species (ROS). Under UV or visible light, photocatalysts, such as TiO_2 or $BiOI/BiVO_4$ heterojunctions, generate electron–hole pairs; the holes oxidize surface hydroxyl groups or water to produce hydroxyl radicals (–OH), while the electrons reduce O_2 to superoxide (O_2^-), some of which further evolve into –OH and H_2O_2.[133,147,148]

Mechanistically, these ROS abstract labile C–H atoms from the polyolefin backbone to yield polyethylene alkyl radicals (PE^-), which rapidly react with dissolved O_2 to form peroxy radicals ($PE–OO^-$). Subsequent propagation steps include hydrogen abstraction from adjacent chains (yielding hydroperoxides, PE–OOH) and β-scission events that cleave C–C bonds, generating carbonyl-containing products, such as aldehydes, ketones, and carboxylic acids, which can be further oxidized to CO_2 and H_2O.[144,147,149]

Termination occurs when two radicals combine (for example, $PE–OO^- + PE–OO^-$ → non-radical products) or when radicals react with ROS, yielding stable oxygenated functionalities. The efficiency of this radical chain depends on light intensity and wavelength, oxygen availability, and polymer morphology. For example, photocatalytic TiO_x-based systems show that HDPE microparticles are attacked mainly by –OH, whereas superoxide plays a lesser role, and the presence of persulfate dramatically enhances ROS generation and fragmentation.[144,147]

12.2. Polyolefin photooxidation scheme (simplified)

PE → (under $h\nu/TiO_2$) → –OH → PE^- → (with O_2) → $PE–OO^-$ → (by abstracting H from another PE chain) → PE–OOH → (β-scission) → ketones, acids, $CO_2 + H_2O$.

This scheme highlights the sequence: light-driven photocatalysis → ROS generation → hydrogen abstraction from backbone → peroxy-radical formation → hydroperoxide formation → β-scission into carbonyl products and eventual mineralization.[147,149]

PET hydrolysis network:

$$\text{PET} \rightarrow (\text{with } H_2O, \text{ at temperature } T) \rightarrow \text{BHET} + \text{oligomers} \rightarrow \text{MHET} \rightarrow \text{TPA} + \text{EG},$$

includes both abiotic and enzymatic nodes, with enzymatic arrows indicating a surface-to-bulk transition: surface-localized PET hydrolysis, followed by solution-phase hydrolysis of oligomers. Recent simulations and enzyme-pathway analyses show that TPA and EG are the dominant low-carbon products, although repolymerization and intermediate rearrangements can occur.[142,146]

12.3. Mechanistic pathways of polyolefin photooxidation and PET hydrolysis in microplastic degradation: from backbone cleavage to mineralization and monomer recovery

Microplastics derived from polyolefins, such as polyethylene (PE) and polyesters like polyethylene terephthalate (PET), exhibit pronounced environmental persistence in aquatic systems, primarily because of the high bond energies of C–C and ester linkages and the semi-crystalline structures that limit access to water, oxygen, and reactive species. In polyolefin-based microplastics, photo- and thermo-oxidative ageing are initiated by hydroxyl radicals generated under UV or visible light *via* semiconductor photocatalysts (such as TiO_2), which abstract hydrogen from the backbone, leading to alkyl and peroxy radicals, hydroperoxide formation, and subsequent β-scission into carbonyl-rich fragments that can be progressively oxidized to CO_2 and H_2O. In parallel, PET undergoes stepwise hydrolysis, either abiotically at elevated temperature or enzymatically at surfaces, *via* a repeated esterolytic motif, first yielding bis-(2-hydroxyethyl) terephthalate (BHET) and oligomers, then mono-(2-hydroxyethyl) terephthalate (MHET), and ultimately terephthalic acid (TPA) and ethylene glycol (EG) as key monomers.[142,146,147,150–153]

Recent advances in photocatalytic PET upcycling and enzymatic PET hydrolysis have shown that these pathways can be

tuned to drive either partial valorization (such as into organic acids, esters, or H_2) or full depolymerization back to monomers suitable for closed-loop recycling. When combined with insights from studies on molecular dynamics and mechanistic design, these reaction networks clarify how bond energies, backbone architecture, and crystallinity jointly modulate the balance between polymer persistence and fragmentation and how the resulting degradation products, ranging from microplastic fragments and hydroperoxides to monomers and organic acids, contribute to ecotoxicological stress in aquatic environments. Embedding these mechanistic schemes into sustainable-management strategies thus enables the design of advanced photocatalytic treatment trains and targeted chemical-recycling routes that can simultaneously reduce microplastic loads and minimize the ecological footprint of plastic pollution in water bodies.[142,150,151,153–157]

12.4. Polyolefin photooxidation scheme (simplified)

(1) Polyethylene (PE) is irradiated in the presence of a photocatalyst (for example, TiO_2) under UV or visible light:

PE + light ($h\nu$) → photocatalyst activation
→ generation of hydroxyl radical (–OH).

(2) The hydroxyl radical abstracts a hydrogen atom from the PE backbone:

OH + PE–H → H_2O + PE^- (polyethylene alkyl radical).

(3) The alkyl radical reacts rapidly with molecular oxygen:

PE^- + O_2 → $PE–OO^-$ (polyethylene peroxy radical).

(4) The peroxy radical abstracts a hydrogen atom from an adjacent PE chain:

$PE–OO^-$ + PE′–H → PE–OOH + PE'^-
(hydroperoxide formation plus a new alkyl radical).

(5) The hydroperoxide undergoes β-scission, breaking the carbon chain:

PE–OOH → ketones + aldehydes + carboxylic acids
+ smaller radical fragments.

(6) The carbonyl products (ketones, aldehydes, acids) are further oxidized: ketones/aldehydes/acids + further oxidation → CO_2 + H_2O (eventual mineralization). Overall conceptual pathway:

PE → ($h\nu$/TiO_2, –OH) → PE^- → $PE–OO^-$ → PE–OOH →
(β-scission) → ketones, aldehydes, carboxylic acids
→ CO_2 + H_2O.

12.5. PET hydrolysis network

(1) PET undergoes hydrolysis in the presence of water and heat (abiotic or catalyst-assisted):

PET + H_2O → bis(2-hydroxyethyl) terephthalate (BHET)
+ oligomers.

(2) BHET and oligomers are further hydrolyzed:

BHET + H_2O → mono(2-hydroxyethyl) terephthalate (MHET).

(3) MHET is hydrolyzed to monomers:

MHET + H_2O → terephthalic acid (TPA) + ethylene glycol (EG).

(4) Enzymatic pathways follow a similar sequence but typically start with surface-localized attack on solid PET:

Solid PET (surface) → surface-bound oligomers →
BHET/MHET in solution → MHET → TPA + EG.

12.5.1 Conceptual network. PET → (H_2O, heat, or enzyme) → BHET + oligomers → MHET → TPA + EG. (12.5.1)

Dominant reaction pathways for microplastic degradation in aquatic environments differ by polymer class, primarily initiated by ROS (such as –OH from photo-Fenton or UV), leading to oxidation, chain scission, and eventual mineralization. PE and PP favour hydrogen-transfer scission over depolymerization, while PS undergoes ring opening, PET hydrolysis, and PVC dechlorination, all enhanced by hydrophilicity gain.[102,137,158]

12.6. Schematic overview

Polymer → initiation (ROS/O_2) → propagation → termination
(mineralization/fragments) (12.6.)

PE/PP (alkene C–C):

Hydro peroxidation → β-scission (k > deploy by $10^3\times$) →
aldehydes → CO_2 (ref. 158)

PS (aromatic):

Carbonyl formation → side-chain oxidation → ring opening
→ benzoquinones[137]

PET (ester):

Hydrolysis (PETase/MHETase) → EG + TPA → β-oxidation[102]

Table 5 Experimentally validated microbial agents for polymer and microplastic biodegradation under laboratory and environmental conditions

Microbes	Isolation source	Polymer type	Degradation time/ extent	Experimental conditions	Degradation confirmed by	Reference
Bacillus cereus	Plastic-dump soil (India)	High-impact polystyrene (HIPS)	30 days/20% weight loss	MSM medium, 26.8 °C, and 120 rpm shaking	FTIR – functional group changes (C=O, O–H peaks); SEM – surface erosion, pits, biofilm	109 and 160
Bacillus paramycoides	Plastic-rich dumpsite soil	Low-density polyethylene (LDPE)	30 days/~20% weight loss	Minimal medium and shaker culture	FTIR – oxidation peaks; SEM – cracks, colonization	161 and 162
Bacillus cereus L1	Plastic-contaminated wastewater (Pakistan)	Low-density polyethylene (LDPE) beads	28 days/19–20% weight loss (1.08 to 0.87 g)	MSM medium, 37 °C, 120 rpm, and UV-pretreated	FTIR – carbonyl (1715 cm^{-1}), alkyne/ nitrile peaks; SEM – pits, cracks	108
Bacillus velezensis GUIA	Deep-sea cold seep	Polyester polyurethane (water-borne)	30 days/significant film degradation	Marine medium, cold conditions	Weight loss; oxidoreductase enzyme activity (Oxr-1)	107
Aspergillus flavus PEDX3	Gut of wax moth (*Galleria mellonella*)	High-density polyethylene (HDPE) microplastics	30 days/surface degradation	Gut isolate culture	FTIR – functional group changes	106
Bacillus cereus	River biofilm on polystyrene (India)	Polystyrene (PS) MPs	30 days/20% weight loss	MSM, 26–28 °C, shaking	FTIR – C=O, O–H formation; SEM – erosion, biofilm	109 and 160
Alcanivorax sp.	Marine plastic debris/seawater	Aliphatic polyesters (PCL, PHB/V, PBS)	Variable/enzyme-mediated	Seawater, pressure-tolerant	Growth profiles; esterase activity	163

PVC (C–Cl):

Dehydrochlorination → polyene
→ crosslinking/aromatization[159]

12.7. Pathway variations

PE and PP exhibit thermal/pyrolytic hydrogen-transfer chain scission as the fastest route (energy barrier-aligned rates), with depolymerization negligible even at high temperatures. PS photoaging *via* ROS yields quinone-like products through aromatic ring disruption, contrasting the HCl loss of PVC, forming conjugated polyenes prone to further oxidation. PET uniquely leverages hydrolases for monomer release, bypassing extensive ROS for aquatic biodegradation.[102,137,158,159]

12.8. Mechanistic clarity

Aquatic pathways unify under basic autoxidation (initiation–propagation–termination), but polymer-specific bonds dictate rates: C–C scission in polyolefins (PE/PP) *vs.* ester cleavage in polyesters (PET). Sequential depolymerization-to-scission occurs dynamically, with ROS lowering barriers for fragmentation before microbial mineralization (Table 5).[137,158]

13. Analytical techniques and limitations in microplastic degradation monitoring

Microplastic degradation involves complex abiotic and biotic processes that alter polymer structures, such as chain scission, oxidation, and fragmentation into nanoplastics, monitored through spectroscopic and pyrolytic methods. Fourier transform infrared (FTIR) spectroscopy identifies chemical signatures by detecting vibrational modes in the infrared range, revealing degradation *via* shifts in carbonyl (C=O around 1700–1750 cm^{-1}), hydroxyl (O–H around 3400 cm^{-1}), and C–H stretching bands, indicative of oxidation and hydrolysis in polymers like polyethylene (PE) and polypropylene (PP). Raman spectroscopy complements FTIR spectroscopy by providing molecular fingerprints through inelastic light scattering, spotting changes like increased fluorescence quenching or peak broadening in degraded polystyrene (PS) from aromatic ring disruptions around 1000 cm^{-1}. Pyrolysis-gas chromatography-mass spectrometry (Py-GC-MS) pyrolyzes particles at 600 °C, separating and identifying degradation products, such as specific monomers (such as styrene from PS at m/z 104) or oligomers, quantifying mass loss in complex matrices.[67,116,164,165] These techniques track degradation but face significant limitations.

FTIR and Raman analyses have detection thresholds around 10–20 μm due to diffraction limits, struggling with nanoplastics below 1 μm where signals drown in noise. Matrix interference from organic matter, water, or salts broadens peaks and reduces signal-to-noise ratios, often requiring pre-processing like density separation or enzymatic digestion that risks particle loss. Nanoplastics identification is particularly challenging; Py-GC-MS achieves ppb sensitivity but is destructive, contamination-prone, and less specific for overlapping pyrolyzates in mixed samples, while FTIR/Raman spectroscopies suffer Mie scattering distortions for sub-20 μm particles. Overall, while FTIR spectroscopy excels for bulk oxidized signatures, Raman spectroscopy for wet samples, and Py-GC-MS for quantification, their combined use is essential yet hampered by high costs, long time (hours per sample), and lack of standardization, limiting field-deployable degradation studies. Future advances in hyperspectral imaging and machine learning could mitigate these issues for more reliable tracking of environmental microplastic breakdown.[67,70,116,164,166,167]

13.1. Radical pathways in microplastic photodegradation and oxidation

Microplastic degradation *via* radical pathways in photodegradation and oxidation relies on reactive oxygen species generated through light-activated processes and catalytic enhancements. These mechanisms break down persistent polymers like polyethylene and polystyrene into smaller fragments or minerals.

13.2. Photodegradation pathways

Photodegradation is initiated when UV light excites chromophores in microplastics, producing polymer radicals that propagate *via* oxygen addition to form peroxy radicals. These undergo autoxidation, creating chain scissions and oxygenated products like carbonyls, with propagation involving hydroperoxide formation and termination by radical coupling. Certain factors, such as light wavelength, oxygen availability, and humidity, accelerate this by enhancing radical mobility and diffusion. Aromatic microplastics like polystyrene further generate triplet excited states (^{3}MNP*) under UV, boosting hydroxyl radical (–OH) production for intensified chain breakdown.[133,168]

13.3. Oxidation mechanisms

Thermal or advanced oxidation processes amplify radical attack, with hydrothermal-Fenton systems achieving 95.9% weight loss in polyethylene microplastics over 16 hours through –OH-dominated cleavage. Here, chain unfolding precedes oxidation, reducing crystallinity and forming carbonyls *via* hydroperoxide intermediates. Hydroxyl radicals from H_2O_2 decomposition target C–H bonds, yielding CO_2 mineralization up to 75.6%. Singlet oxygen ($^1O_2$) and superoxide also contribute to photo-oxidative cycles, fragmenting aliphatic polymers like polypropylene.[111,169]

13.4. Sensitizer functions

Photosensitizers extend light absorption, with aged polystyrene microplastics generating environmentally persistent free radicals, $^1O_2$, and triplet states that degrade co-pollutants 12 times faster than pristine forms. Algal extracellular polymeric substances act as sensitizers under sunlight, producing ^{3}EPS*, $^1O_2$, and O_2^- to accelerate polystyrene aging, increasing surface

hydroxyls and dissolved organic release. Nanomaterial sensitizers like dye-modified TiO_2 enhance charge separation, tripling polyethylene breakdown by transferring excitation energy to substrate radicals.[133,170]

13.5. Transition metal catalysis

Iron-based Fenton catalysts generate –OH *via* Fe^{2+}–H_2O_2 reactions, enabling two-stage microplastic hydrolysis–oxidation with high efficiency across polyethylene variants. Multivalent metals (Fe, Cu, Co) activate peroxides in Fenton-like systems, producing ROS for polymer chain scission, with polymer-supported Fe_3O_4 composites maintaining stability over cycles. TiO_2 and ZnO, often metal-doped, form heterojunctions that separate electron–hole pairs for sustained –OH and $^1O_2$ generation, degrading polystyrene up to 98%.[111,116,133,171,172]

13.6. Degradation implications

These radical pathways reduce microplastic persistence, but intermediates may heighten toxicity until mineralization. Optimized conditions, such as acidic pH, hydrothermal aid, and modified catalysts, maximize efficiency while minimizing by-products. Future designs should target visible-light sensitizers and stable metal composites for scalable aquatic remediation.[111,133,169,173]

13.7. Polyethylene (PE) mechanisms

Polyethylene, a prevalent polyolefin in packaging, primarily undergoes photo-oxidative degradation under UV light, initiating chain scission and carbonyl formation that embrittles the material. Mechanical forces like abrasion then fragment it into smaller particles, while bio-deterioration by bacteria, such as *Rhodococcus ruber*, involves surface fouling, enzymatic oxidation *via* laccases, and hydrolysis of weakened bonds. Studies confirm the slow breakdown of PE, with oxidation products leaching additives and enabling microbial penetration after months of exposure.[126,174,175]

13.8. Polypropylene (PP) pathways

Similar to PE, polypropylene experiences dominant photodegradation, where UV radiation cleaves C–C bonds, generating radicals that cross-link or fragment the chain, reducing tensile strength. Thermal aging accelerates this in warmer environments, promoting volatilization of low-molecular-weight fractions, followed by microbial assimilation by fungi like *Aspergillus* species through exoenzymes that erode the surface. Research highlights the resistance of PP, with degradation rates lagging behind those of polyethylene, owing to its branched structure.[116,126,174,175]

13.9. Polystyrene (PS) breakdown

Polystyrene, common in foams, degrades *via* photolysis under sunlight, producing styrene monomers and oxidized groups that increase hydrophilicity for biofilm formation. Mechanical stress from waves causes brittle fracture, while biotic hydrolysis by esterase-like enzymes from *Pseudomonas* spp. targets degraded segments, yielding oligomers. Expanded PS shows faster initial fragmentation but persistent micro-scale residues.[126,139,176,177]

13.10. Polyethylene terephthalate (PET) processes

PET bottles degrade through the hydrolytic cleavage of ester linkages, accelerated by alkaline conditions and enzymes like PETase from *Ideonella sakaiensis*, which depolymerizes it to terephthalic acid and ethylene glycol. UV exposure precedes this by creating microcracks, enhancing enzyme access, although full mineralization remains limited without consortia.[177,178]

13.11. Polyvinyl chloride (PVC) dynamics

PVC undergoes dehydrochlorination under UV light or heat, forming conjugated polyene sequences that cause discoloration and embrittlement, ultimately leading to mechanical fragmentation. Biodegradation remains minimal, primarily involving dehalogenases from marine bacteria (*e.g.*, actinobacteria) that cleave C–Cl bonds to release chloride ions, though this is slow and limited. Phthalate plasticizers leach readily from PVC, increasing polymer accessibility but not directly facilitating biodegradation.[175]

13.12. Polyurethane (PU) degradation

Polyurethanes fragment *via* the hydrolysis of urethane bonds under humid conditions, with oxidative enzymes from fungi like *Phanerochaete chrysosporium* cleaving soft segments. Photo-oxidation generates quinones, promoting microbial adhesion (Table 6).[126,178]

14. Polymer backbone structures in microplastics

Polymer backbone structures fundamentally dictate the degradation resistance of common microplastics like polyethylene (PE), polypropylene (PP), polystyrene (PS), and polyethylene

Table 6 Summary of the physiological factors

Polymer class	Abiotic-dominant	Biotic-dominant
PE and PP	Photo-oxidation and mechanical	Enzymatic oxidation and biofragmentation
PS	Photolysis and mechanical	Hydrolysis and biofouling
PET	Hydrolysis and UV cracking	PETase hydrolysis
PVC	Dehydrochlorination	Chloridase action
PU	Hydrolysis and photo-oxidation	Urethane cleavage

Table 7 Evaluation of microplastic treatment technologies across efficiency, energy demand, life-cycle impacts, and operational constraints[98,104,111,116,119,121–123,126,174,182–193]

S. no.	Parameters	Enzymatic/microbial degradation	Photocatalysis/advanced oxidation processes	Conventional physical–chemical removal
1	Typical MP removal/ degradation efficiency	Engineered strains and enzymes can achieve high conversion of PET and other polyesters under optimized lab conditions but often at slow rates in real waters	UV/H_2O_2, thermal Fenton, and semiconductor photocatalysis frequently show >80–90% mass loss of selected MPs within hours in controlled reactors	Coagulation–flocculation, membrane filtration, and adsorption routinely remove >70–95% of suspended MPs from wastewater without chemical mineralization
2	Mineralization *vs.* fragmentation	Biodegradation can ultimately mineralize MPs to CO_2 and biomass, although complete mineralization is rarely quantified and is substrate-dependent	AOPs and photocatalysis can partially mineralize MPs but often leave oxidized fragments and dissolved organics unless reaction times and oxidant doses are very high	Physical methods mainly concentrate and separate MPs without altering polymer chemistry, so no mineralization occurs
3	Selectivity and by-product toxicity	High substrate selectivity; metabolic intermediates are usually low-toxicity monomers and biomass, providing low risk of toxic oxidation by-products	Non-selective ROS attack can generate small oxidized organics and radical species with ecotoxicity concerns for aquatic biota	Coagulants, flocculants, or sorbents may introduce chemical residues and spent media that require further handling but do not generate ROS-derived by-products
4	Energy demand	Operates under conditions of mild temperature and no external light, but fermentation and aeration can still consume significant energy at scale	UV lamps, pressurized reactors, and oxidant generation impose high energy footprints unless solar or waste heat is leveraged	Settling, filtration, and flotation are comparatively energy-moderate; some membrane and advanced filtration systems still require substantial pumping energy
5	Greenhouse gas and life-cycle impacts	LCA studies suggest low direct emissions, but upstream burdens from nutrient media, bioreactors, and enzyme production can be non-trivial	AOP LCAs indicate notable carbon and chemical footprints due to oxidant manufacture, lamp operation, and catalyst synthesis	Physical removal often shows favourable life-cycle performance when integrated into existing treatment trains but raises issues of MP concentrate disposal
6	Operational conditions (pH, *T*, salinity)	Many enzymes operate in narrow pH/temperature windows and can be inhibited by salinity, surfactants, and heavy metals common in real waters	AOPs tolerate broader pH and salinity ranges, but performance still declines with radical scavengers and high organic loads	Coagulation and filtration are robust to variable water matrices when optimized and are already standardized for municipal use
7	Scalability and infrastructure needs	Large-scale application requires controlled bioreactors or biofilm reactors and stable inocula, which are still under development for MPs	Scaling photocatalytic/AOP reactors for large flow rates is technically feasible but capital-intensive, with unresolved issues of catalyst recovery and reactor fouling	Physical removal fits directly into existing drinking-water and wastewater plants, making it currently the most industrially viable option
8	Treatment timescales	Biodegradation often requires days to weeks for substantial mass loss, especially for crystalline PE and PP MPs	Many AOPs achieve significant degradation within minutes to hours, making them suitable as rapid pre-treatments	Physical methods act instantaneously at the hydraulic retention time of the treatment unit but do not reduce polymer persistence if leaks occur
9	Polymer-type dependence	Highly effective for hydrolysable polymers (PET, some polyesters, polyurethanes) but far less efficient for non-polar PE/PP unless pre-oxidized	Capable of degrading a broad spectrum (PE, PP, PS, PET) because radical attack is non-selective, although rates depend strongly on crystallinity and size	Removal efficiency is mainly size- and density-dependent, with limited discrimination among polymer chemistries

Table 7 (*Contd.*)

S. no.	Parameters	Enzymatic/microbial degradation	Photocatalysis/advanced oxidation processes	Conventional physical–chemical removal
10	Risk of secondary nano-plastic formation	Slow surface erosion can still generate smaller particles, but progressive biodegradation tends to further metabolize fragments over time	Aggressive AOPs can initially increase nano- and micro-fragment formation before eventual oxidation, posing transient exposure risks	Mechanical stresses in filtration and pumping may also fragment MPs; however, most fragments remain captured in sludge streams
11	Catalyst/agent recovery and reuse	Microbial cells self-replicate, but maintaining activity and preventing escape of engineered strains requires containment; enzyme immobilization is an active research area	Heterogeneous catalysts (TiO_2, doped oxides, supported metals) must be recovered to avoid nanoparticle release and remain economically viable	Coagulant sludge and spent filters demand disposal or regeneration; sorbents like activated carbon can be thermally regenerated but at an energy cost
12	Co-benefits for other pollutants	Certain microbial consortia can simultaneously degrade dissolved organics and some additives or plasticizers	AOPs efficiently oxidize co-occurring pharmaceuticals, dyes, and endocrine disruptors along with MPs	Physical methods co-remove suspended solids, algae, and some sorbed contaminants, improving overall water clarity
13	Ecological compatibility and risk	Engineered microbes and enzymes must be contained to avoid unintended ecological impacts, but well-designed systems can be highly benign	ROS exposure, catalyst leaching, and transformation products require careful ecotoxicological evaluation before environmental deployment	Existing technologies already operate under regulatory oversight; additional risk is mostly associated with sludge handling rather than new chemistries
14	Integration into treatment trains	Enzymes and selected microbial reactors are promising as polishing stages following the physical concentration of MPs	Photocatalytic/AOP steps are often proposed as pre-oxidation or tertiary polishing units, coupled with biological or membrane processes	Coagulation, sedimentation, and membranes form the core MP removal units in many proposed treatment trains, with advanced units added as needed
15	Technology readiness and near-term deployment	Microbial and enzyme-based MP degradation is at pilot scale at best, with intense ongoing work on enzyme engineering and reactor design	AOPs and photocatalysis have several full-scale analogues in drinking-water and wastewater treatment, but MP-specific implementations are still emerging	Conventional removal is already deployed globally, making it the immediate backbone for MP control while more advanced degradation technologies improve

terephthalate (PET), with bond energies, crystallinity, and additives playing pivotal roles in their environmental persistence.

14.1. Structural variations and degradation resistance

PE and PP feature all-carbon (C–C) backbones composed of long hydrocarbon chains, where strong C–C ($\approx$348 kJ mol^{-1}) and C–H ($\approx$413 kJ mol^{-1}) bonds render them highly inert to hydrolysis and microbial attack, primarily degrading *via* photo-oxidation that initiates radical chain scission only after prolonged UV exposure. In contrast, PS shares a similar C–C backbone but incorporates bulky phenyl side groups that sterically hinder chain mobility and enzymatic access, further elevating its stability, while the ester linkages of PET (C–O–C, $\approx$358 kJ mol^{-1}) introduce hydrolyzable heteroatoms, enabling faster abiotic and biotic breakdown compared with polyolefins. These structural variances mean that PE and PP microplastics, often from packaging, persist for centuries in marine and soil environments, fragmenting into nanoplastics rather than mineralizing, whereas PET fragments from bottles degrade more readily under enzymatic catalysis like PETase.[102,119,159,179,180]

14.2. Role of bond energies in degradation kinetics

Bond energies directly influence degradation kinetics: the high dissociation energy of C–C bonds in PE, PP, and PS demands energy-intensive initiation steps, such as UV photolysis, forming peroxyl radicals that propagate oxidation but rarely achieve complete mineralization without synergism from oxidants like ozone or H_2O_2. The weaker ester bonds of PET, however, succumb to nucleophilic attack under neutral or alkaline conditions, accelerating hydrolysis and reducing molecular weight from millions to oligomers within months under optimal lab conditions.

14.3. Crystallinity and additive effects

Crystallinity amplifies this resistance; higher degrees in PE (up to 60–80%) and PP create densely packed, impermeable regions that exclude water, oxygen, and microbes, slowing diffusion-limited degradation by orders of magnitude compared with amorphous zones. For instance, low-crystallinity PET ($T_g \approx 70$ °C) exhibits 70% mass loss in enzymatic assays at 50 °C, but crystalline domains resist penetration, prolonging persistence. Additives exacerbate these effects: antioxidants like hindered phenols in PE/PP scavenge radicals, extending lifespan 2–5-fold, while plasticizers in PS leach out, embrittling the matrix and paradoxically hastening fragmentation without true biodegradation. Heavy metal stabilizers in PVC (although less relevant here) or UV absorbers in PET similarly modulate photodegradation pathways, often yielding persistent by-products like carboxylic acids.[102,119,159,180,181]

Overall, these factors interplay to make polyolefin microplastics dominant in global pollution inventories, with degradation favouring fragmentation over dissolution, posing ecological risks *via* bioaccumulation. Mitigation strategies target additive removal and crystallinity reduction *via* pre-processing, yet field rates remain low, underscoring the need for redesigned polymers with labile backbones (Table 7).[176,178,180,181]

15. Viable WWTP-integrated technologies

Viable technologies for microplastic removal in wastewater treatment plants (WWTPs) include primary sedimentation, coagulation–flocculation, and membrane-based systems, which achieve 50–99% removal efficiencies and are already integrated into full-scale operations. Laboratory-scale approaches, such as advanced photocatalysis and certain bio-electrochemical systems, show promise but lack scalability owing to high costs and stability issues. Catalyst stability metrics, like recyclability over 5–10 cycles with minimal leaching (<1.5 mg per L iron), are critical for practical adoption, although many remain unproven at scale.[38,184,194–196]

Conventional WWTP processes effectively capture microplastics (MPs) during primary treatment through sedimentation and screening, removing 50–78% of particles larger than 50 μm. Coagulation–flocculation, often using ferric chloride or alum, enhances this to 95–99% efficiency by aggregating MPs into settleable flocs, as demonstrated in Beijing WWTPs with air circulation and anaerobic–anoxic–oxic (A2O) stages. These methods are cost-effective, require minimal retrofitting, and handle high-throughput flows (such as 100 000 m^3 day^{-1}), making them viable for global integration.[38,130,195]

Secondary treatments like activated sludge and membrane bioreactors (MBRs) further boost removal to 87–99%, trapping MPs in biomass flocs or ultrafiltration membranes (0.01–0.1 μm pores). Rapid sand filtration and disc filters as tertiary add-ons achieve >95% removal of residual MPs <10 μm, with full-scale pilots in Europe showing sustained performance over the years. Hybrid MBR-reverse osmosis (RO) systems treat gray water for reuse, separating MPs *via* biomass filtration followed by salt/organic rejection.[38,195,197,198]

15.1. Laboratory-scale proof-of-concepts

Photocatalytic degradation using TiO_2 or Fe_2O_3–MnO_2 micromotors remains lab-confined, mineralizing MPs *via* reactive oxygen species; it is limited by UV dependency and low quantum yields (<10% at scale). Metal–organic frameworks (MOFs), like Zr-based foams or FeS_2/C nano catalysts, adsorb/degrade MPs in batch reactors (such as 98% fluoxetine proxy removal), yet face fouling and energy demands precluding WWTP pilots.[130,184,194]

TAML/peroxide activators and bio-electrochemical wetlands degrade MPs in controlled setups (26–98% micropollutant reduction), but sludge handling and land needs hinder upscale. Solar-driven convection *via* glass spheres fuses MPs into blocks without chemicals, achieving lab efficiencies >90%, although throughput is <1 L h^{-1}. Zn–Al layered double hydroxides (LDHs) adsorb nanoplastics in freshwater mimics, but regeneration cycles fail beyond three runs.[184,198,199]

15.2. Catalyst stability metrics

Stability is quantified by leaching rates, cycle durability, and activity retention; such as FeS_2/C catalysts leach <1.5 mg per L Fe^{2+} over 6 hours, retaining >80% activity post-use *via* core–shell pyrite structures. Recyclability benchmarks include 5–10 cycles with <10% degradation, as in graphene oxide-intercalated FeOF, which removes 76.9% neonicotinoids after regeneration (*vs.* 18.6% untreated spent catalyst).[194,196]

Photocatalysts like Fe_2O_3–MnO_2 micromotors maintain 90% efficiency over five cycles through adsorptive bubble separation but aggregate beyond 10 runs. MOF-derived pyrite shows superior pyrite baselines, with N-doping enhancing Fenton-like –OH generation and mass transport *via* nano-porous carbon. Metrics emphasize pH stability (near-neutral 6–8) and mineralization (TOC reduction >70%), critical for WWTPs.[184,194,199]

15.3. Integration challenges and outlook

WWTP integration favours low-energy, retrofit-compatible methods like disc filters over energy-intensive catalysis. Natural coagulants (such as Moringa–alum hybrids) offer 99.8% removal sustainably but vary with biomass quality. Future hybrids, such as AOPs post-MBR, could address nanoplastics, prioritizing catalysts with >90% retention after 20 cycles (Table 8).[38,130,196]

16. Advances in microplastic degradation: assessing the scalability of emerging technologies

Microplastic (MP) pollution has become a global environmental crisis due to the extreme persistence of synthetic polymers in aquatic, terrestrial, and atmospheric systems, driving intense research into degradation technologies over the past decade. Recent reviews highlight that MPs can be attacked through

Table 8 Comparison of technologies

Technology	Scale	MP removal (%)	Stability/recyclability	Key limitation
Coagulation–flocculation	Full-scale WWTP	95–99%	>100 cycles; no leaching	Small MPs (<10 μm)[130]
MBR + sand filtration	Full-scale	87–99%	Membrane lifespan: 5–10 years	Fouling/energy[195]
Photocatalysis (TiO_2)	Lab	80–95%	3–5 cycles; 20% loss	UV needs[184]
FeS_2/C electro-Fenton	Pilot/lab	90–98%	>6 hours; <1.5 mg L^{-1} leach	Cost[194]
TAML/H_2O_2	Lab	26–98%	Continuous dose; scalable proj.	Optimization[199]
MOF micromotors	Lab	>90%	5 cycles; adsorption-based	Throughput[184]

abiotic routes, such as photodegradation, thermal oxidation, and advanced oxidation processes (AOPs), and through biotic pathways involving bacteria, fungi, and engineered enzymes. Abiotic methods often rely on UV-light-driven photocatalysis or Fenton-like reactions to generate reactive oxygen species (ROS) that break polymer chains into smaller organics and, ideally, mineralize them to CO_2 and H_2O. For example, TiO_2-based photocatalysts and peroxide-assisted AOPs have achieved MP removal efficiencies in the range of ≈30–95% under controlled laboratory conditions, suggesting strong potential for engineered water-treatment trains. However, these systems remain largely at pilot or bench scale, with challenges around catalyst recovery, energy input, and the formation of partially oxidized intermediates that may retain ecotoxicity.[116,126,174,200–203]

Biological approaches, particularly microbial and enzymatic degradation, have gained prominence as more "green" alternatives. Bacteria such as *Pseudomonas* spp. and fungi like *Aspergillus* and *Fusarium* strains have been shown to adhere to polyethylene (PE) and polyethylene terephthalate (PET) surfaces, secrete extracellular enzymes (such as cutinases, esterases, and laccases), and progressively depolymerize MPs into lower-molecular-weight fragments and monomers. Recent work using synthetic-biology tools, including CRISPR-based engineering, has improved enzyme–substrate affinity and turnover rates for PET and other polyesters, raising expectations for tailored biocatalysts. Despite these advances, most microbial and enzymatic systems are still confined to laboratory proof-of-concept studies, with degradation times spanning weeks to months and limited validation in complex environmental matrices, such as seawater or wastewater sludge. Scale-up is further hindered by sensitivity to temperature, pH, and competing organic matter, and concerns about the unintended ecological impacts of releasing engineered microbes.[104,123,126,174,204,205]

Among the approaches reviewed, AOP-based and photocatalytic systems appear most promising for near-term scale-up, especially when integrated into existing wastewater-treatment infrastructure, because they operate on relatively short timescales and can be engineered into flow-through reactors. In contrast, microbial and enzymatic biodegradation remain largely at the laboratory stage, requiring significant optimization of consortia, enzyme stability, and process economics before deployment at full scale. Hybrid strategies, such as combining adsorption on bio-based or porous frameworks (such as cellulose–MOF composites) with *in situ* photocatalysis, offer a pragmatic bridge, concentrating MPs and then degrading them in a single unit operation, but their long-term durability and techno-economic viability still need field-level validation. Overall, while no single technology yet provides a complete, universally applicable solution, AOP- and photocatalysis-driven routes are the closest to scalable deployment, whereas biotechnological methods represent a longer-term, high-potential pathway contingent on advances in enzyme engineering and environmental risk assessment.[104,123,126,174,200,202–204]

17. Research gaps

Despite promising advancements in microplastic degradation techniques, significant challenges persist in achieving efficient, scalable, and environmentally safe solutions. Chemical and advanced oxidation processes often generate toxic by-products, while biological methods suffer from slow kinetics and incomplete mineralization. Recent reviews emphasize the need for standardized protocols and deeper mechanistic insights to bridge these gaps.

To detect and model the toxic effects of microplastics (MPs) and nanoplastics (NPs) in aquatic systems, several critical methodological gaps must be addressed to ensure reliable, reproducible findings. These include deficiencies in kinetic modelling frameworks, absence of uniform testing protocols, difficulties validating results in realistic environmental matrices, persistent limitations in NP detection, and insufficient exploration of synergistic stressor interactions like temperature, salinity, and UV exposure.[64,206–208]

17.1. Gaps in kinetic modelling

Kinetic models for MP transport, degradation, and bioaccumulation often oversimplify dynamic processes, such as fragmentation, biofouling, and vertical mixing. Many rely on two-dimensional assumptions that neglect depth-dependent settling or turbulent diffusion, leading to inaccurate predictions of MP distribution in stratified water columns. For instance, models frequently exclude macroplastic-to-microplastic breakdown rates or particle shape variability, which influence settling velocities by up to 50% in coastal zones. Statistical models, while computationally efficient, suffer from uncertain inputs like beaching probabilities and lack integration of biological uptake kinetics, hindering their predictive power for long-term exposure scenarios.[207]

Future efforts must prioritize three-dimensional hydrodynamic models incorporating real-time biofouling data and field-

calibrated degradation constants. Without these advancements, kinetic simulations cannot reliably forecast MP hotspots in rivers or estuaries, undermining risk assessments for aquatic biota.

17.2. Lack of standardized testing conditions

Ecotoxicity studies on MPs/NPs vary widely in terms of particle characterization, dispersion method, and exposure duration, complicating comparisons across datasets. No universal guidelines exist for reporting polymer type, size distribution, surface chemistry, or aging status, resulting in exposure concentrations that span orders of magnitude (such as 1 μg L^{-1} to 10 g L^{-1}). Dispersants like sodium azide in commercial NP suspensions introduce artifacts, masking true particle effects and inflating apparent toxicity.[209]

Standardization initiatives, such as those proposed for OECD guidelines, should mandate dynamic light scattering for size verification, zeta potential measurements for stability, and positive controls with known toxicants like potassium dichromate. Replicate consistency is vital given the aggregation tendencies of MPs, yet many protocols overlook matrix-matched controls, perpetuating inter-laboratory discrepancies of over 200% in LC_{50} values.

17.3. Challenges in real-matrix validation

Laboratory assays typically use clean water, ignoring complex environmental matrices like sediments, biofilms, or dissolved organics that alter MP bioavailability. In real aquatic samples, humic acids and salts promote NP aggregation, reducing uptake by 30–70% compared with synthetic media, while validation against field data remains rare owing to sampling inconsistencies. Techniques like Raman spectroscopy achieve high accuracy (>96%) in spiked waters but falter in sediments where spectral noise from clays overwhelms NP signals.[64,210]

Real-matrix validation demands integrated approaches: sequential digestion-filtration for sample prep, coupled with machine learning-enhanced spectroscopy for quantification down to 10^5 particles per L. Cross-platform calibration with certified reference materials is essential, yet only a few studies report recovery efficiencies below 80% in marine sediments, highlighting a pressing need for harmonized protocols.[210]

17.4. Nanoplastics detection limitations

NPs (<1 μm) evade conventional detection because of optical diffraction limits and low signal-to-noise ratios in FTIR/Raman spectroscopies, with practical thresholds around 200–500 nm even in advanced setups. Matrix interferences exacerbate this, as proteins and minerals quench fluorescence or cause nonspecific binding, while exhaustive sample prep (such as density separation) risks particle loss exceeding 50%. Emerging nanodevices like SERS substrates offer sub-100 nm resolution but lack field portability and standardized calibration.[64]

Progress hinges on hybrid methods like nano-FTIR with ML classification that bypass separation steps, yet reproducibility testing and inter-lab comparisons are scarce. Regulatory acceptance awaits robust reference materials mimicking environmental NPs, currently limiting their integration into monitoring frameworks.

17.5. Combined stressor effects

The aquatic toxicity of MPs intensifies under combined stressors, where elevated temperature (such as +5 °C) accelerates the leaching of additives like phthalates 2–3-fold, while salinity fluctuations (10–35 ppt) modulate aggregation and biofilm formation. UV exposure synergizes with heat to photooxidize polymers, enhancing hydrophilicity and bioavailability, but protective biofilms at higher salinities can attenuate this by 40%. Multi-stressor studies reveal antagonistic effects: low salinity boosts oil-MP toxicity (LC_{50} < 1 μg per L PAH equivalents), yet few dissect NP-specific interactions across trophic levels.[206]

Comprehensive factorial designs are needed, simulating realistic gradients (such as 20–30 °C, 15–35 ppt, UV 5–20 W m^{-2}) to capture non-linear interactions. Current gaps in multi-stressor kinetics impede accurate environmental risk modelling.[207]

Methodological inconsistencies dominate current studies on microplastic degradation. Experimental designs vary widely in polymer types, particle sizes, UV exposure, temperature, and agitation, hindering the comparability and reproducibility of results. For instance, aquatic degradation tests rarely simulate realistic conditions like synergistic abiotic–biotic interactions, leading to the overestimation or underestimation of field rates.[116,193]

Biological degradation faces kinetic limitations, with microbial and enzymatic processes achieving only 0–15% weight loss over 0–3 months for common polymers like polyethylene (PE) and polypropylene (PP). Fungi and bacteria, such as *Aspergillus niger* and *Pseudomonas* sp., show potential against PE and PET, but efficiency drops under conditions of natural salinity, low temperatures, or nutrient scarcity. Toxic intermediates from incomplete breakdown pose secondary pollution risks, particularly in marine systems.[126,211,212]

Chemical methods like photocatalysis with TiO_2 yield high weight loss (up to 78% for LDPE), yet produce reactive oxygen species harmful to aquatic life. Enzymatic approaches, including PETase and cutinases, excel on PET but falter on recalcitrant PP and PVC owing to poor stability, pH sensitivity, and scalability issues. Nanoplastics, formed from microplastic fragmentation, evade most treatments, amplifying long-term risks in food chains and human tissues.[211–213]

Toxicological data gaps exacerbate concerns. Microplastics adsorb persistent pollutants, transferring them *via* trophic levels, yet long-term ecological and human health impacts remain underexplored. Bioplastics, touted as alternatives, degrade slowly in aquatic environments, often matching conventional plastics and releasing additives.[183,214]

18. Conclusions

Microplastic pollution originates from diverse anthropogenic sources beyond primary plastic manufacturing, encompassing

textile fibres, cosmetic microbeads, and wastewater effluents. These contaminants permeate multiple environmental matrices, including marine systems, terrestrial soils, glacial deposits and human biological compartments, underscoring their ubiquitous distribution. Although physical, chemical and biological degradation approaches have been extensively investigated, no methodology has achieved complete, environmentally benign mineralisation at industrially relevant scales. Advances in microbial consortia development and enzyme engineering demonstrate potential, yet current degradation efficiencies remain inadequate for practical remediation. The regulatory framework for plastic waste management in India exemplifies the imperative for globally harmonised, evidence-based policies emphasising prevention over end-of-pipe treatment.

19. Future directions

Standardised experimental protocols incorporating consistent parameters, which are polymer compositions, particle dimensions, exposure periods and realistic environmental matrices, must be prioritised to enhance reproducibility and enable robust predictive modelling. The genetic engineering of microbial strains and enzymes, facilitated by metagenomics, directed evolution and synthetic biology, holds transformative potential. Such approaches could elevate degradation rates to nearly complete polymer mineralisation within hours under ambient conditions.

Synergistic microbial consortia comprising bacteria, fungi and algae merit systematic investigation. These multi-species assemblages are expected to outperform mono-cultures through complementary metabolic pathways and interspecies synergies. Concurrently, the deployment of advanced wastewater treatment technologies engineered for microplastic capture prior to effluent discharge represents a critical intervention. Comprehensive life-cycle assessments of bioplastic alternatives must accompany these developments to preclude unintended ecological consequences.

Hybrid systems integrating advanced oxidation processes with photocatalysis warrant optimisation using tailored catalysts, such as ZnO and GO/TiO_2 composites, to maximise degradation whilst minimising secondary pollutant formation. Long-term studies elucidating nanoplastic persistence, trophic transfer and toxicological endpoints across ecosystems and human health endpoints are urgently required.

Sustainable microplastic governance necessitates alignment with circular economy principles, encompassing biodegradable polymer innovation, regulatory restrictions on single-use plastics, textile microfibres and microbeads, alongside targeted public education campaigns. International collaboration and equitable environmental policy frameworks will prove essential for achieving meaningful pollution abatement and ecosystem preservation.

Author contributions

Conceptualization, investigation and supervision were performed by D. S. Material preparation, data collection, analysis and manuscript preparation were performed by S. K. S. All authors read and approved the final manuscript.

Conflicts of interest

The authors declare that they have no known competing financial interests or personal relationships that could have appeared to influence the work reported in this paper.

Data availability

No primary research results, software or code have been included, and no new data were generated or analysed as part of this review.

Acknowledgements

The authors Dhanaraj Sangeetha and Shivani Kumar gratefully acknowledge the Vellore Institute of Technology, India, for providing the seed grant support (SG20230132) and the research facilities (VIT CRF).

References

1 P. G. C. Nayanathara Thathsarani Pilapitiya and A. S. Ratnayake, *Cleaner Mater.*, 2024, **11**, 100220.
2 R. Dallaev, N. Papež, M. M. Allaham and V. Holcman, *Polymers*, 2025, **17**, 1981.
3 H. Jung, G. Shin, H. Kwak, L. T. Hao, J. Jegal, H. J. Kim, H. Jeon, J. Park and D. X. Oh, *Chemosphere*, 2023, **320**, 138089.
4 M. Bel Hassen, A. Bellaaj Zouari, M. Abdennadher, J.-C. Assaf, M. Nakad, R. Abboud, Y. Khammeri, M. Banni, A. Panzeri, L. Gomes and W. Hamd, *Front. Environ. Sci.*, 2025, **13**, 1635230.
5 E. Guzzetti, A. Sureda, S. Tejada and C. Faggio, *Environ. Toxicol. Pharmacol.*, 2018, **63**, 1.
6 S. Lambert and M. Wagner, *Freshwater Microplastics*, 2018, p. 1.
7 B. Chae, S. Oh and D. G. Lee, *Mar. Pollut. Bull.*, 2023, **196**, 115591.
8 C. B. Yuen, H. L. Chong, M.-H. Kwok and T. Ngai, *Sustain. Food Technol.*, 2025, **3**, 908–929.
9 K. T. Ho, R. Bjorkland and R. M. Burgess, *Mar. Pollut. Bull.*, 2024, **207**, 116907.
10 O. Setälä, V. Fleming-Lehtinen and M. Lehtiniemi, *Environ. Pollut.*, 2014, **185**, 77–83.
11 D. S. Green, B. Boots, N. E. O'Connor and R. Thompson, *Environ. Sci. Technol.*, 2017, **51**, 68–77.
12 S. Mehra, K. Sharma, G. Sharma, M. Singh and P. Chadha, in *Emerging Contaminants*, IntechOpen, 2021.
13 V. Prakash, S. Dwivedi, K. Gautam, M. Seth and S. Anbumani, *Environ. Chem. Sustainable World*, 2020, 223.
14 L. Lebreton, B. Slat, F. Ferrari, B. Sainte-Rose, J. Aitken, R. Marthouse, S. Hajbane, S. Cunsolo, A. Schwarz, A. Levivier, K. Noble, P. Debeljak, H. Maral,

R. Schoeneich-Argent, R. Brambini and J. Reisser, *Sci. Rep.*, 2018, **8**, 4666.
15 G. Pellini, A. Gomiero, T. Fortibuoni, C. Ferrà, F. Grati, A. N. Tassetti, P. Polidori, G. Fabi and G. Scarcella, *Environ. Pollut.*, 2018, **234**, 943–952.
16 T. S. Galloway, M. Cole and C. Lewis, *Nat. Ecol. Evol.*, 2017, **1**, 0116.
17 J. Gigault, A. ter Halle, M. Baudrimont, P. Y. Pascal, F. Gauffre, T. L. Phi, H. El Hadri, B. Grassl and S. Reynaud, *Environ. Pollut.*, 2018, **235**, 1030–1034.
18 S. Klein, E. Worch and T. P. Knepper, *Environ. Sci. Technol.*, 2015, **49**, 6070–6076.
19 H. S. Auta, C. U. Emenike and S. H. Fauziah, *Environ. Int.*, 2017, **102**, 165–176.
20 M. Revel, A. Châtel and C. Mouneyrac, *Current Opinion in Environmental Science & Health*, 2018, **1**, 17–23.
21 M. Paul, *Microplastics in 90% Frogs Studied in Bangladesh Delta, Can Threaten Biodiversity: Study*, Bangladesh, 2023.
22 A. Ragusa, A. Svelato, C. Santacroce, P. Catalano, V. Notarstefano, O. Carnevali, F. Papa, M. C. A. Rongioletti, F. Baiocco, S. Draghi, E. D'Amore, D. Rinaldo, M. Matta and E. Giorgini, *Environ. Int.*, 2021, **146**, 106274.
23 H. A. Leslie, M. J. M. van Velzen, S. H. Brandsma, A. D. Vethaak, J. J. Garcia-Vallejo and M. H. Lamoree, *Environ. Int.*, 2022, **163**, 107199.
24 S. Bandopadhyay, L. Martin-Closas, A. M. Pelacho and J. M. DeBruyn, *Front. Microbiol.*, 2018, **9**, 819.
25 M.-P. Belioka and D. S. Achilias, *Water Emerging Contam. Nanoplast.*, 2024, **3**, 09.
26 O. Ahmad, M. Jamal, H. Almalki, A. Alzahrani, A. Alatawi and M. Haque, *Journal of Advanced Veterinary and Animal Research*, 2025, **12**, 260.
27 S. Zhao, K. F. Kvale, L. Zhu, E. R. Zettler, M. Egger, T. J. Mincer, L. A. Amaral-Zettler, L. Lebreton, H. Niemann, R. Nakajima, M. Thiel, R. P. Bos, L. Galgani and A. Stubbins, *Nature*, 2025, **641**, 51–61.
28 T. Thiemann, *J. Water Resour. Prot.*, 2025, **17**, 159–195.
29 T. Kaviarasan, K. Dhineka, M. Sambandam, S. K. Sivadas, D. Sivyer, D. Hoehn, U. Pradhan, P. Mishra and M. V. Ramana Murthy, *Ocean Coast Manag.*, 2022, **223**, 106177.
30 H. Kye, J. Kim, S. Ju, J. Lee, C. Lim and Y. Yoon, *Heliyon*, 2023, **9**, e14359.
31 M. Branka, *Global Journal of Ecology*, 2023, **8**, 064–074.
32 *Regional Plastics Outlook for Southeast and East Asia*, OECD Publishing, 2025.
33 M. I. Hossain, Y. Zhang, A. N. M. A. Haque and M. Naebe, *Materials*, 2025, **18**, 2513.
34 I. E. Napper and R. C. Thompson, *Glob. Chall.*, 2020, **4**, 1900081.
35 E. AlShamaileh and M. Alzoubi, *Sci. Prog.*, 2025, **108**, 368504251376048.
36 J. Lv, T. Huang, B. Wu, X. Hu, Y. Ding and Y. Zhang, *Sci. Rep.*, 2025, **15**, 31405.
37 M. Komorowska-Kaufman and W. Marciniak, *Desalination Water Treat.*, 2024, **317**, 100006.
38 T. Reza, Z. H. Mohamad Riza, S. R. Sheikh Abdullah, H. Abu Hasan, N. 'Izzati Ismail and A. R. Othman, *Toxics*, 2023, **12**, 12.
39 V. P. Kasa, A. K. S. V. Brahmandam, B. Samal, V. R. S. Cheela, B. K. Dubey and K. Pathak, *Sci. Total Environ.*, 2025, **959**, 178339.
40 D. Yona, P. Nooraini, S. E. N. Putri, S. H. J. Sari, R. A. Lestariadi and A. Amirudin, *Front. Mar. Sci.*, 2023, **10**, 1220650.
41 J. Song, C. Wang and G. Li, *ACS ES&T Water*, 2024, **4**, 2330–2332.
42 A. Šaravanja, T. Pušić and T. Dekanić, *Materials*, 2022, **15**, 2683.
43 J. Chen, W. Wang, H. Liu, X. Xu and J. Xia, *Environ. Pollut. Bioavailab.*, 2021, **33**, 227–246.
44 Y. Wang, G. Liu, Y. Wang, H. Mu, X. Shi, C. Wang and N. Wu, *Toxics*, 2023, **11**, 539.
45 S. K. Mishra, T. Sanyal, P. Kundu, R. Kumar, D. Ghosh, G. Chakrabarti, N. Sikdar, S. Bhattacharya, S. Paul and A. Das, *Mol. Cancer*, 2025, **24**, 248.
46 T. Wang, D. Liu, R. Liu, F. Yuan, Y. Ding, J. Tao, Y. Wang, W. Yu, Y. Fang and B. Li, *Environ. Sci. Technol.*, 2025, **59**, 7667–7677.
47 M. J. Stapleton and F. I. Hai, *Bioengineered*, 2023, **14**, 2244754.
48 K. Tadsuwan and S. Babel, *J. Environ. Chem. Eng.*, 2022, **10**, 107142.
49 S. Ittisupornrat, C. Namyuang, A. Phetrak, P. Sriromreun and S. Theepharaksapan, *Front. Microbiol.*, 2025, **16**, 1519230.
50 H. Miera-Domínguez, P. Lastra-González, I. Indacoechea-Vega and D. Castro-Fresno, *Road Mater. Pavement Des.*, 2024, **25**, 1658–1679.
51 M. Zhang, H. Yin, J. Tan, X. Wang, Z. Yang, L. Hao, T. Du, Z. Niu and Y. Ge, *Atmos. Environ.*, 2023, **297**, 119597.
52 A. Rani, *J. Polym. Mater.*, 2022, **39**, 17–35.
53 L. Apete, O. V. Martin and E. Iacovidou, *Mar. Pollut. Bull.*, 2024, **205**, 116530.
54 O. Ahmad, M. Jamal, H. Almalki, A. Alzahrani, A. Alatawi and M. Haque, *Journal of Advanced Veterinary and Animal Research*, 2025, **12**, 260.
55 A. I. Osman, M. Hosny, A. S. Eltaweil, S. Omar, A. M. Elgarahy, M. Farghali, P.-S. Yap, Y.-S. Wu, S. Nagandran, K. Batumalaie, S. C. B. Gopinath, O. D. John, M. Sekar, T. Saikia, P. Karunanithi, M. H. M. Hatta and K. A. Akinyede, *Environ. Chem. Lett.*, 2023, **21**, 2129–2169.
56 N. Razeghi, A. H. Hamidian, C. Wu, Y. Zhang and M. Yang, *Environ. Chem. Lett.*, 2021, **19**, 4225–4252.
57 L. Lv, X. Yan, L. Feng, S. Jiang, Z. Lu, H. Xie, S. Sun, J. Chen and C. Li, *Water Environ. Res.*, 2021, **93**, 5–15.
58 H. Almuhtaram and R. C. Andrews, *ACS ES&T Water*, 2022, **2**, 1276–1278.
59 J.-T. Lin, Y.-P. Chung, Y.-Y. Lee, T.-L. Wu, T. T. T. Huynh, P. T. Nguyen, M.-J. Lu, B.-W. Huang, B. Sriram, S.-F. Wang, G.-P. Chang-Chien, S. Kogularasu and W.-C. Lin, *Talanta Open*, 2025, **12**, 100514.

60 P. A. Todd, C. L. X. Yong, S. H. Foo, L. S. M. Ying and J. Ledet, *Front. Mar. Sci.*, 2024, **11**, 1345591.
61 V. Hidalgo-Ruz, L. Gutow, R. C. Thompson and M. Thiel, *Environ. Sci. Technol.*, 2012, **46**, 3060–3075.
62 J.-T. Lin, Y.-P. Chung, Y.-Y. Lee, T.-L. Wu, T. T. T. Huynh, P. T. Nguyen, M.-J. Lu, B.-W. Huang, B. Sriram, S.-F. Wang, G.-P. Chang-Chien, S. Kogularasu and W.-C. Lin, *Talanta Open*, 2025, **12**, 100514.
63 J. Workman, *Spectroscopy*, 2024, ac7567r4.
64 R. P. Debri, F. Sepe, S. Romano, N. D'Orazio, A. De Lorenzo, A. Calarco, R. Conte and G. Peluso, *Nanomaterials*, 2025, **16**, 55.
65 A. Arredondo-Navarro, X. Wang, K. Hess, D. Gallardo-Owens, E. El Hayek, J. M. Cerrato and J. Gonzalez-Estrella, *Environ. Eng. Sci.*, 2025, **42**, 505–510.
66 L. D. B. Mandemaker and F. Meirer, *Angew. Chem., Int. Ed.*, 2023, **62**, e202210494.
67 N. P. Ivleva, *Chem. Rev.*, 2021, **121**, 11886–11936.
68 B. Ardini, L. Pittura, A. Frontini, M. Benedetti, S. Gorbi, F. Regoli, G. Cerullo, G. Valentini and C. Manzoni, *Environ. Sci. Technol.*, 2025, **59**, 9255–9264.
69 C. Rauert, N. Charlton, A. Bagley, S. A. Dunlop, C. Symeonides and K. V. Thomas, *Environ. Sci. Technol.*, 2025, **59**, 1984–1994.
70 J. Kumar, P. Amulraj, S. F. Haroon, R. Selvasembian, V. R. Soma and R. Panneerselvam, *iScience*, 2025, **28**, 113888.
71 Y. Umurhan, M. Songsart-Power, T. B. Limbu and T. Phan, *Environ. Sci. Pollut. Res.*, 2025, **32**, 28630–28677.
72 M. Dong, Q. Zhang, X. Xing, W. Chen, Z. She and Z. Luo, *Sci. Total Environ.*, 2020, **739**, 139990.
73 D. S. Mendes, D. N. N. Silva, M. G. Silva, C. R. Beasley and M. E. B. Fernandes, *Sci. Rep.*, 2024, **14**, 29044.
74 A. G. López, R. G. Najjar, M. A. M. Friedrichs, M. A. Hickner and D. H. Wardrop, *Front. Mar. Sci.*, 2021, **8**, 715924.
75 L. Hartz, L. Grabinski and S. Salameh, *Front. Environ. Sci.*, 2025, **13**, 1600570.
76 H. Yang, G. Chen and J. Wang, *Toxics*, 2021, **9**, 41.
77 L. Huang, S. Zhang, L. Li, S. Zhang, J. Wang, X. Liu and W. Zhang, *Polar Sci.*, 2023, **36**, 100946.
78 A. Tursi, M. Baratta, T. Easton, E. Chatzisymeon, F. Chidichimo, M. De Biase and G. De Filpo, *RSC Adv.*, 2022, **12**, 28318–28340.
79 D. Pal, R. Prabhakar, V. B. Barua, I. Zekker, J. Burlakovs, A. Krauklis, W. Hogland and Z. Vincevica-Gaile, *Environ. Sci. Pollut. Res.*, 2024, **32**, 56–88.
80 T. L. Jolaosho, M. F. Rasaq, E. V. Omotoye, O. V. Araomo, O. S. Adekoya, O. Y. Abolaji and J. J. Hungbo, *Ecotoxicol. Environ. Saf.*, 2025, **294**, 118036.
81 U. R. Gurjar, K. A. M. Xavier, S. P. Shukla, S. Takar, A. K. Jaiswar, G. Deshmukhe and B. B. Nayak, *Mar. Pollut. Bull.*, 2023, **187**, 114545.
82 E. Marcharla, S. Vinayagam, L. Gnanasekaran, M. Soto-Moscoso, W.-H. Chen, S. Thanigaivel and S. Ganesan, *Environ. Res.*, 2024, **256**, 119181.
83 M. N. Issac and B. Kandasubramanian, *Environ. Sci. Pollut. Res.*, 2021, **28**, 19544–19562.
84 M. Saisanthosh Vamshi Harsha, P. Abhiram Siva Prasad and D. Bhanu Prakash, *IgMin Research*, 2024, **2**, 460–468.
85 M. H. Kudzin, M. Gloc, N. Festinger-Gertner, M. Sikora and M. Olak-Kucharczyk, *Toxics*, 2025, **13**, 928.
86 H. Zhong, M. Wu, C. Sonne, S. S. Lam, R. W. M. Kwong, Y. Jiang, X. Zhao, X. Sun, X. Zhang, C. Li, Y. Li, G. Qu, F. Jiang, H. Shi, R. Ji and H. Ren, *Eco-Environ. & Health*, 2023, **2**, 142–151.
87 A. Witczak, L. Przedpełska, K. Pokorska-Niewiada and J. Cybulski, *Toxics*, 2024, **12**, 571.
88 F. C. C. G. of I. Central Pollution Control Board and Ministry of Environment, *Plastic Waste Management Rules*, 2022, accessed: Dec. 26, 2025 [Online], https://cpcb.nic.in/uploads/plasticwaste/2-amendment-pwmrules-2022.pdf.
89 N. Bhardwaj, India's New Plastic Waste Management Rules Effective from July 1, 2022, India Briefing, Jun. 30, 2022.
90 D. Pal, R. Prabhakar, V. B. Barua, I. Zekker, J. Burlakovs, A. Krauklis, W. Hogland and Z. Vincevica-Gaile, *Environ. Sci. Pollut. Res.*, 2024, **32**, 56–88.
91 M. C. Ariza-Tarazona, J. F. Villarreal-Chiu, V. Barbieri, C. Siligardi and E. I. Cedillo-González, *Ceram. Int.*, 2019, **45**, 9618–9624.
92 T. S. Tofa, K. L. Kunjali, S. Paul and J. Dutta, *Environ. Chem. Lett.*, 2019, **17**, 1341–1346.
93 F. Miao, Y. Liu, M. Gao, X. Yu, P. Xiao, M. Wang, S. Wang and X. Wang, *J. Hazard. Mater.*, 2020, **399**, 123023.
94 Y. Tang, S. Zhang, Y. Su, D. Wu, Y. Zhao and B. Xie, *Chem. Eng. J.*, 2021, **406**, 126804.
95 J. Zhao, Y. Ruan, Z. Zheng, Y. Li, M. Sohail, F. Hu, J. Ling and L. Zhang, *iScience*, 2023, **26**, 106823.
96 X. Zhang, M. Zhang, C. Luo, Y. Li, L. Zhang, C. Li, X. Zhang, J. Liao and W. Zhou, *Appl. Catal. B Environ. Energy*, 2025, **371**, 125288.
97 M. Zandieh, E. Griffiths, A. Waldie, S. Li, J. Honek, F. Rezanezhad, P. Van Cappellen and J. Liu, *Exploration*, 2024, **4**, 20230018.
98 P. Pfohl, M. Wagner, L. Meyer, P. Domercq, A. Praetorius, T. Hüffer, T. Hofmann and W. Wohlleben, *Environ. Sci. Technol.*, 2022, **56**, 11323–11334.
99 M. C. Ariza-Tarazona, J. F. Villarreal-Chiu, J. M. Hernández-López, J. Rivera De la Rosa, V. Barbieri, C. Siligardi and E. I. Cedillo-González, *J. Hazard. Mater.*, 2020, **395**, 122632.
100 A. Sharara, M. Samy, M. Mossad and M. Gar Alalm, *Environ. Sci. Pollut. Res.*, 2023, **31**, 3951–3963.
101 Smriti, J. P. Kushwaha and N. Singh, *J. Environ. Chem. Eng.*, 2025, **13**, 119017.
102 Z. Cai, M. Li, Z. Zhu, X. Wang, Y. Huang, T. Li, H. Gong and M. Yan, *Microorganisms*, 2023, **11**, 1661.
103 A. L. G. Cavalcante, D. N. Dari, M. F. de Morais Silva, R. da Silva Vieira, F. I. da Silva Aires, P. G. de Sousa, K. M. dos Santos and J. C. S. dos Santos, *Mol. Catal.*, 2025, **585**, 115392.
104 G. K. Gupta, M. Dixit, E. Chot and P. Shukla, *ACS Environ. Au*, 2025, **5**, 520–542.
105 F. Alidoosti, M. Giyahchi and H. Moghimi, *Curr. Res. Microb. Sci.*, 2025, **9**, 100450.

106 J. Zhang, D. Gao, Q. Li, Y. Zhao, L. Li, H. Lin, Q. Bi and Y. Zhao, *Sci. Total Environ.*, 2020, **704**, 135931.
107 Z. Gui, G. Liu, X. Liu, R. Cai, R. Liu and C. Sun, *Microbiol. Spectr.*, 2023, **11**, e00073.
108 S. S. Iqbal, Y. Rehman, M. Afzaal, S. Ali, S. A. Al-Hussain, R. Nawaz, I. Nasim, A. Irfan and M. E. A. Zaki, *Microb. Cell Fact.*, 2025, **24**, 238.
109 S. Kumari, S. Nagpal, S. Ali Khan and C. Chinglenthoiba, DOI:DOI: 10.20517/eceh.2025.08.
110 X. Duan, Z. Ning, X. Sui, S. Geng, H. Wang, C. Liu and L. Chang, *J. Environ. Chem. Eng.*, 2025, **13**, 116207.
111 K. Hu, P. Zhou, Y. Yang, T. Hall, G. Nie, Y. Yao, X. Duan and S. Wang, *ACS ES&T Eng.*, 2022, **2**, 110–120.
112 G. Sourkouni, C. Kalogirou, P. Moritz, A. Gödde, P. K. Pandis, O. Höfft, S. Vouyiouka, A. A. Zorpas and C. Argirusis, *Ultrason. Sonochem.*, 2021, **76**, 105627.
113 D. Hu, Z. Wu, J. Huang and G. Zhang, *ACS ES&T Water*, 2025, **5**, 5614–5622.
114 T. Liu, W. Wang, D. Yu, X. Zhu, J. Li and Y. Wang, *Appl. Energy*, 2025, **391**, 125805.
115 M.-H. Cho, Y.-J. Song, C.-J. Rhu and B.-R. Go, *Polymers*, 2023, **15**, 241.
116 S. Yousafzai, M. Farid, M. Zubair, N. Naeem, W. Zafar, Z. ul Zaman Asam, S. Farid and S. Ali, *Environ. Sci. Adv.*, 2025, **4**, 1142–1165.
117 Y. Xu, Q. Ou, J. P. van der Hoek, G. Liu and K. M. Lompe, *Environ. Sci. Technol.*, 2024, **58**, 991–1009.
118 Y. Xiao, Y. Tian, W. Xu and J. Zhu, *Materials*, 2024, **17**, 2755.
119 N. Mohanan, Z. Montazer, P. K. Sharma and D. B. Levin, *Front. Microbiol.*, 2020, **11**, 580709.
120 M. Surana, D. S. Pattanayak, V. Yadav, V. K. Singh and D. Pal, *Environ. Res.*, 2024, **247**, 118268.
121 K. J. Ramírez-Escárcega, K. J. Amaya-Galván, J. C. García-Prieto, F. d. J. Silerio-Vázquez and J. B. Proal-Nájera, *J. Environ. Chem. Eng.*, 2025, **13**, 115594.
122 E. Mbuci Kinyua, G. W. Atwoki Nyakairu, E. Tebandeke and O. N. Odume, *Advances in Environmental and Engineering Research*, 2023, **04**, 1–21.
123 J. Choi, H. Kim, Y.-R. Ahn, M. Kim, S. Yu, N. Kim, S. Y. Lim, J.-A. Park, S.-J. Ha, K. S. Lim and H.-O. Kim, *RSC Adv.*, 2024, **14**, 9943–9966.
124 S. Mateo, A. Zhang, A. Piedra, A. Ruiz, R. Miranda and F. Rodríguez, *ACS ES&T Water*, 2024, **4**, 3049–3058.
125 S.-Y. Ren and H.-G. Ni, *Toxics*, 2023, **11**, 432.
126 P. Yadav, A. Kumar, K. Ram, A. Kumar, R. K. Gupta and L. Dufossé, *Curr. Res. Microb. Sci.*, 2025, **9**, 100495.
127 A. Ccanccapa-Cartagena, A. N. Gopakumar and M. Salehi, *MethodsX*, 2025, **14**, 103173.
128 R. Kaegi, M. Philipp, I. S. Jüngling, N. P. Ivleva and T. D. Bucheli, *Anal. Bioanal. Chem.*, 2025, **417**, 6191–6208.
129 M. Webb, J. Buckman, B. Ratouit, J. Scott, J. Bischoff, T. T. Le, T. Gutierrez, T. Wagner, H. T. T. Ngo, M. Kaiser and R. Pereira, *Sci. Rep.*, 2025, **15**, 44361.
130 A. K. Badawi, R. Hasan and B. Ismail, *RSC Adv.*, 2025, **15**, 25256–25273.
131 W. Wohlleben, M. Rückel, L. Meyer, P. Pfohl, G. Battagliarin, T. Hüffer, M. Zumstein and T. Hofmann, *Environ. Sci. Technol. Lett.*, 2023, **10**, 698–704.
132 C. S. S. Reddy, B. Ganesh and S. Jeyachandran, *Asian J. Chem.*, 2025, **37**, 2355–2365.
133 E. Mbuci Kinyua, G. W. Atwoki Nyakairu, E. Tebandeke and O. N. Odume, *Advances in Environmental and Engineering Research*, 2023, **04**, 1–21.
134 A. G. Stancu, M. Râpă, C. L. Popa, S. I. Donţu, E. Matei and C. I. Covaliu-Mirelă, *Molecules*, 2025, **30**, 3186.
135 I. Nabi, A.-U.-R. Bacha, K. Li, H. Cheng, T. Wang, Y. Liu, S. Ajmal, Y. Yang, Y. Feng and L. Zhang, *iScience*, 2020, **23**, 101326.
136 J. Duan, Y. Li, J. Gao, R. Cao, E. Shang and W. Zhang, *Water Res.*, 2022, **216**, 118320.
137 X. Shi, Z. Chen, X. Liu, W. Wei and B.-J. Ni, *Sci. Total Environ.*, 2022, **846**, 157498.
138 S. Lyu, J. Zhang, B. Pudil and D. Untereker, *Does Crystallinity Affect Polymer Degradation Rates?*.
139 S. S. Ali, T. Elsamahy, R. Al-Tohamy and J. Sun, *Environ. Sci. Ecotechnology*, 2024, **21**, 100427.
140 G. Wang, Z. Zhang, D. Xu, B. Xing, L. Zhu and S. Wang, *Sci. Total Environ.*, 2023, **897**, 165359.
141 Y. Zhang, D. Yang, X. Li, P.-A. Chen, X. Yao and Z. Jian, *Natl. Sci. Rev.*, 2025, **12**, nwaf489.
142 S. M. Ma, P. Pereira, C. W. Pester, P. E. Savage, B. R. Bakshi and L.-C. Lin, *J. Phys. Chem. B*, 2025, **129**, 6594–6603.
143 J. Qian, X. Li, C. Tang and Z. Qiang, *Macromolecules*, 2025, **58**, 12716–12726.
144 H. Nakatani and A. T. N. Dao, *Molecules*, 2025, **30**, 4461.
145 S. Zeng, D. Lu and R. Yang, *Polymers*, 2024, **16**, 3038.
146 S. Schubert, K. Schaller, J. A. Bååth, C. Hunt, K. Borch, K. Jensen, J. Brask and P. Westh, *ChemBioChem*, 2023, **24**, e202200516.
147 Y. He, A. U. Rehman, M. Xu, C. A. Not, A. M. C. Ng and A. B. Djurišić, *Heliyon*, 2023, **9**, e22562.
148 D. Chu, J. Weng, X. Liu, H. Wang, Y. Cui, L. Nie and Z. Li, *CCS Chem.*, 2025, **7**, 3519–3529.
149 X. Liu, Z. Hu, B. S. Portela, E. M. Rettner, A. Pineda, J. Miscall, N. A. Rorrer, A. T. Krummel, R. S. Paton and G. M. Miyake, *Angew. Chem., Int. Ed.*, 2025, **64**, e202418411.
150 W. Hamd, E. A. Daher, T. S. Tofa and J. Dutta, *Front. Mar. Sci.*, 2022, **9**, 885614.
151 B. Sui, T. Wang, J. Fang, Z. Hou, T. Shu, Z. Lu, F. Liu and Y. Zhu, *Front. Microbiol.*, 2023, **14**, 1265139.
152 R. Wei, G. von Haugwitz, L. Pfaff, J. Mican, C. P. S. Badenhorst, W. Liu, G. Weber, H. P. Austin, D. Bednar, J. Damborsky and U. T. Bornscheuer, *ACS Catal.*, 2022, **12**, 3382–3396.
153 E. Hwang, R. Ahmad, I. Shafique, W. J. Shim, S. Son and S. Kim, *Mar. Pollut. Bull.*, 2026, **222**, 118664.
154 Y. Shi, Z. Yu, S. Bao, X. Yang and Y. Lu, *J. Environ. Chem. Eng.*, 2025, **13**, 117194.
155 S. Kang, W. Yuan, W. Chen, M. Du, Y. Zhang and B. Qiu, *Nanotechnology*, 2023, **34**, 462001.

156 H. Kang, A. Washington, M. D. Capobianco, X. Yan, V. V. Cruz, M. Weed, J. Johnson, G. Johns, G. W. Brudvig, X. Pan and J. Gu, *ACS Mater. Lett.*, 2023, **5**, 3032–3041.
157 S. Jiang, M. Wang, Y. Huang, J. Wen and P. Hu, *ChemSusChem*, 2025, **18**, e202401920.
158 L. Wang, W. Cheng, X. Yang, R. Wang, R. Liu, Y. Zhu, Y. Yi, Y. Tang and Z. Wang, *Polym. Degrad. Stab.*, 2023, **215**, 110450.
159 B. Gewert, M. M. Plassmann and M. MacLeod, *Environ. Sci. Process. Impacts*, 2015, **17**, 1513–1521.
160 W. Wang, S. Yao, Z. Zhao, Z. Liu, Q. X. Li, H. Yan and X. Liu, *Environ. Pollut.*, 2024, **343**, 123202.
161 S. Thakur, S. Mathur, M. Saraf, S. Patel, R. Jadav and S. Menon, *J. Pure Appl. Microbiol.*, 2025, **19**, 1419–1433.
162 A. Tirkey and L. S. B. Upadhyay, *Environ. Sci. Adv.*, 2025, **4**, 952–963.
163 V. Zadjelovic, A. Chhun, M. Quareshy, E. Silvano, J. R. Hernandez-Fernaud, M. M. Aguilo-Ferretjans, R. Bosch, C. Dorador, M. I. Gibson and J. A. Christie-Oleza, *Environ. Microbiol.*, 2020, **22**, 1356–1369.
164 A. M. Othman, A. A. Elsayed, Y. M. Sabry, D. Khalil and T. Bourouina, *ACS Omega*, 2023, **8**, 10335–10341.
165 E. Dümichen, P. Eisentraut, C. G. Bannick, A.-K. Barthel, R. Senz and U. Braun, *Chemosphere*, 2017, **174**, 572–584.
166 E. Dümichen, P. Eisentraut, C. G. Bannick, A.-K. Barthel, R. Senz and U. Braun, *Chemosphere*, 2017, **174**, 572–584.
167 J. Timarac-Popović, J. Hiesberger, E. Šesto, N. Luhmann, A. Giesriegl, H. Bešić, J. P. Lafleur and S. Schmid, *arXiv*, 2026, preprint, arXiv:2504.10192, DOI: 10.48550/arXiv.2504.10192.
168 Y. Xu, Q. Ou, J. P. van der Hoek, G. Liu and K. M. Lompe, *Environ. Sci. Technol.*, 2024, **58**, 991–1009.
169 Y. Xiao, Y. Tian, W. Xu and J. Zhu, *Materials*, 2024, **17**, 2755.
170 F. Li, X. Bai, Y. Ji and M. Kang, *J. Hazard. Mater.*, 2024, **469**, 133949.
171 B. Bouzayani and M. Á. Sanromán, *Molecules*, 2024, **29**, 2188.
172 Y. Liu and J. Wang, *Chem. Eng. J.*, 2023, **466**, 143147.
173 A. Sun and W.-X. Wang, *Environ. Sci. Technol.*, 2025, **59**, 5223–5236.
174 P. R. Sutkar, R. D. Gadewar and V. P. Dhulap, *J. Hazard. Mater. Adv.*, 2023, **11**, 100343.
175 X. Zhong, L. Qiang, J. Cheng, Z. Sun, H. Hu, H. Liu and R. Zhang, *Appl. Soil Ecol.*, 2025, **215**, 106394.
176 Y.-D. Lin, P.-H. Huang, Y.-W. Chen, C.-W. Hsieh, Y.-L. Tain, B.-H. Lee, C.-Y. Hou and M.-K. Shih, *Toxics*, 2023, **11**, 747.
177 B. Thakur, J. Singh, J. Singh, D. Angmo and A. P. Vig, *Sci. Total Environ.*, 2023, **877**, 162912.
178 X. Yao, X. Yang, Y. Lu, Y. Qiu and Q. Zeng, *Polymers*, 2024, **17**, 66.
179 M. Lewanska and R. Barczynska, *Polymers*, 2025, **17**, 2923.
180 X. Zhang, Z. Yin, S. Xiang, H. Yan and H. Tian, *Polymers*, 2024, **16**, 2807.
181 R. A. Clark and M. P. Shaver, *Chem. Rev.*, 2024, **124**, 2617–2650.
182 R. De Jesus and R. Alkendi, *Front. Microbiol.*, 2023, **13**, 1066133.
183 M. A. A. Amparán, A. Palacios, G. M. Flores and P. M. C. Olivera, *Environ. Monit. Assess.*, 2025, **197**, 429.
184 Y. Pan, S.-H. Gao, C. Ge, Q. Gao, S. Huang, Y. Kang, G. Luo, Z. Zhang, L. Fan, Y. Zhu and A.-J. Wang, *Environ. Sci. Ecotechnology*, 2023, **13**, 100222.
185 P. V. Gayathri, S. Joseph, M. Mohan and D. Pillai, *Water Environ. J.*, 2023, **37**, 686–701.
186 T. Rim, Y. Xing, M. Kang, W. Li, Y. Chen, D. Zhang, W. Li, Y. Guo, X. Zhang, S. Wang, Z. Qian, W. Su and B. Jiang, *Environ. Sci.*, 2025, **11**, 2881–2905.
187 M. G. J. Löder, H. K. Imhof, M. Ladehoff, L. A. Löschel, C. Lorenz, S. Mintenig, S. Piehl, S. Primpke, I. Schrank, C. Laforsch and G. Gerdts, *Environ. Sci. Technol.*, 2017, **51**, 14283–14292.
188 M. J. Sawma, R. M. Zayyat, R. Ghaddar and G. M. Ayoub, *Water Emerging Contam. Nanoplast.*, 2024, **3**, 21.
189 H. Jiao, S. S. Ali, M. H. M. Alsharbaty, T. Elsamahy, E. Abdelkarim, M. Schagerl, R. Al-Tohamy and J. Sun, *Ecotoxicol. Environ. Saf.*, 2024, **271**, 115942.
190 Y. Ma, K. Jin, X. Yin, X. Zhao, Z. Liu, Y. Dou, T. Ao, Y. Li and X. Duan, *Desalination Water Treat.*, 2025, **322**, 101135.
191 P. Ebrahimbabaie, K. Yousefi and J. Pichtel, *Sci. Total Environ.*, 2022, **806**, 150603.
192 S. Rawat, S. M. Tauseef and M. Sharma, *Beilstein J. Nanotechnol.*, 2025, **16**, 2144–2167.
193 K. Brožová, S. Heviánková, J. Halfar, K. Čabanová and A. Valigůrová, *Front. Environ. Sci.*, 2025, **13**, 1677793.
194 Z. Ye, J. A. Padilla, E. Xuriguera, J. L. Beltran, F. Alcaide, E. Brillas and I. Sirés, *Environ. Sci. Technol.*, 2020, **54**, 4664–4674.
195 M. S. Nasir, I. Tahir, A. Ali, I. Ayub, A. Nasir, N. Abbas, U. Sajjad and K. Hamid, *Heliyon*, 2024, **10**, e25883.
196 Z. Wan, S. H. Chae, A. F. Meese, O. Nwokonkwo, L. Arrazolo, K. L. Yip, X. Ma, S. Liu, C. Muhich, D. Wang, H. Wei and J.-H. Kim, *Nat. Commun.*, 2025, **16**, 9672.
197 S. Zahmatkesh, K. T. T. Amesho and M. Sillanpää, *J. Hazard. Mater. Adv.*, 2022, **7**, 100121.
198 J. Shamshad and R. Ur Rehman, *Environ. Sci. Adv.*, 2025, **4**, 189–222.
199 Y. Somasundar, M. Park, K. D. Daniels, G. R. Warner, A. D. Ryabov, S. A. Snyder and T. J. Collins, *ACS ES&T Water*, 2021, **1**, 2155–2163.
200 M. Shen, B. Song, C. Zhou, T. Hu, G. Zeng and Y. Zhang, *Sci. Total Environ.*, 2022, **842**, 156723.
201 J. Chen, J. Wu, P. C. Sherrell, J. Chen, H. Wang, W. Zhang and J. Yang, *Advanced Science*, 2022, **9**, 2103764.
202 S. Zhuang, S. Huang, L. Dai, X. Lu, Z. Long and Z. He, *Chem. Eng. J.*, 2025, **524**, 169627.
203 K. Rizwan and M. Bilal, *Environ. Sci. Pollut. Res.*, 2022, **29**, 86933–86953.
204 P. Yadav, C. Yadav, A. Joshi, M. Meena and J. Arora, *Next Research*, 2025, **2**, 100878.
205 Z. Yuan, R. Lv, F. Gudda, A. Mosa, P. Oleszczuk, T. Minkina, Y. Gao and L. Tang, *New Contaminants*, 2025, **1**, 1–10.
206 M. E. DeLorenzo, P. B. Key, K. W. Chung, K. Aaby, D. Hausman, C. Jean, P. L. Pennington, E. C. Pisarski and

E. F. Wirth, *Arch. Environ. Contam. Toxicol.*, 2021, **80**, 461–473.
207 T. Moodley, T. Abunama, S. Kumari, D. Amoah and M. Seyam, *Environ. Monit. Assess.*, 2024, **196**, 667.
208 V. Tolardo, D. Magrì, F. Fumagalli, D. Cassano, A. Athanassiou, D. Fragouli and S. Gioria, *Nanomaterials*, 2022, **12**, 1947.
209 O. Pikuda, E. G. Xu, D. Berk and N. Tufenkji, *Environ. Sci. Technol. Lett.*, 2019, **6**, 21–25.
210 H. Jin, *Transactions on Materials, Biotechnology and Life Sciences*, 2024, **4**, 56–68.
211 Y. Cao, J. Bian, Y. Han, J. Liu, Y. Ma, W. Feng, Y. Deng and Y. Yu, *Toxics*, 2024, **12**, 463.
212 H. Al-Madhagi, *Green Chem. Lett. Rev.*, 2025, **18**, 1–20.
213 D. Rede, C. Delerue-Matos and V. C. Fernandes, *Polymers*, 2023, **15**, 3356.
214 R. C. Thompson, W. Courtene-Jones, J. Boucher, S. Pahl, K. Raubenheimer and A. A. Koelmans, *Science*, 2024, **386**, 274.